The Sigma-1 Receptor as an Atypical Kv1.2 Auxiliary Subunit

By

Madelyn Jean Abraham

A Thesis submitted to the Faculty of Graduate and Postdoctoral Studies
In fulfillment of the requirements for the degree of MSc of Neuroscience

Department of Cellular and Molecular Medicine
Faculty of Medicine
University of Ottawa

ABSTRACT

Delayed-rectifier potassium channels comprised of the Kv1.2 subunit are critical in maintaining appropriate neuronal excitability and determining the threshold for action potential firing. This is attributed in part to the interaction of the Kv1.2 subunit with an unidentified molecule that confers bimodal channel activation gating, allowing neurons to adapt to repetitive trains of stimulation and protecting against hyperexcitability.

It is well established that the Sigma-1 receptor (Sig-1R) regulates members of the Shaker K+ channel family at baseline and upon Sig-1R ligand-activation. While an interaction between Kv1.2 and Sig-1R has been previously demonstrated, the biophysical nature of this interaction has not been elucidated. We hypothesized that Sig-1R may regulate the Kv1.2 biophysical properties and may further act as the unidentified modulator of Kv1.2 activation gating.

To explore the interaction between Kv1.2 and Sig-1R, whole-cell voltage-clamp electrophysiology and apFRET imaging experiments were performed in recombinant HEK293 cells transiently transfected with Kv1.2 and Sig-1R. It was found that ligand-activation of Sig-1R decreases Kv1.2 current amplitude, likely due to a ligand-dependent change in Sig-1R activity rather than increased association of Sig-1R with Kv1.2. Further, we show that Sig-1R interacts with Kv1.2 in baseline conditions to modulate bimodal activation gating.

We show that Sig-1R modulation of Kv1.2 is abolished both in the presence of Kvβ2, a known auxiliary subunit of Kv1.2, and following expression of the Sig-1R mutation underlying ALS16 (Sig-1R-E102Q). These data respectively suggest that Kvβ2 physically occludes the interaction of the Sig-1R with Kv1.2, and that E102 may be a residue critical for efficient Sig-1R modulation of Kv1.2.

Taken together, this data provides novel insights regarding the modulation of neuronal delayed-rectifier potassium channels by Sig-1R. This work provides a new role for Sig-1R in the regulation of neuronal excitability and introduces a mechanism of pathophysiology in Sig-1R dysfunction.

ACKNOWLEDGEMENTS

I would like to thank my supervisor Dr. Richard Bergeron for his support and instruction throughout the completion of my studies.

I would like to express my gratitude to Dr. Adrian Wong for his contribution to experimental design and data analysis; his assistance was essential to the completion of the work within this thesis.

Thank you to Nina Ahlskog, Chloe Stewart, Kieran McCann, and Elitza Hristova for their support and friendship over the entirety of my studies.

I would also like to thank Meagan E. Abraham for generation of multiple schematic representations, Kayla Ferguson for producing a cDNA construct used in this work, and Drs. Johnny Ngsee and Antonio Colavita for their guidance and advice as my Thesis Advisory Committee members.

TABLE OF CONTENTS

LIST OF ABBREVIATIONS

ALS	Amyotrophic Lateral Sclerosis
apFRET	Acceptor-photobleaching FRET
BiP	Binding immunoglobulin protein
CNS	Central nervous system
co-IP	Co-immunoprecipitation
dHMN	Distal hereditary motor neuropathy
EPSP	Excitatory post-synaptic potential
ER	Endoplasmic Reticulum
eYFP	Enhanced Yellow Fluorescent Protein
FBS	Fetal Bovine Serum
FG	Fast Green total protein stain
FRAP	Fluorescence Recovery After Photobleaching
FRET	Fluorescence Resonance Energy Transfer
GFP	Green Fluorescent Protein
GOF	Gain of function
HEK293	Human Embryonic Kidney cells
HSP	Hereditary Spastic Paraplegia
IHC	Immunohistochemistry
iPSC	Induced pluripotent stem cell
IV Plot	Current-Voltage Plot
Kv Channel	Voltage-gated potassium channel
LOF	Loss of function
MAM	Mitochondria associated ER membrane
mCh	m-Cherry
MND	Motor neuron disease
NMDAR	N-methyl-D-aspartate receptors
PBS	Phosphate Buffered Saline
PNS	Peripheral nervous system
PSD95	Postsynaptic density protein 95
RIPA	Radioimmunoprecipitation buffer
ROI	Region of Interest
SEM	Standard Error of the Mean
SGR	Soluble gating regulator
Sig-1R	Sigma-1 Receptor
SKF	SKF-10,047
UPR	Unfolded protein response
YFP	Yellow Fluorescent Protein

LIST OF FIGURES

LIST OF TABLES

1. INTRODUCTION

1.1 Voltage-Gated Potassium Channels

1.1.1 Overview

Voltage-gated potassium channels (Kv channels) comprise an extensive and well-studied gene superfamily. In mammals, Kv channels are coded for by at least 22 different genes, with additional varieties of channels created via alternative splicing (Yellen, 2002) and RNA editing (Jan and Jan, 2012). Electrophysiological characterization has revealed that, although structurally similar, Kv channels are functionally diverse: they may be inwardly or outwardly rectifying, rapidly or slowly inactivating, and may interact with numerous modulatory auxiliary proteins. The functional diversity of Kv channels contributes to the varied physiological roles of different neuronal types and different neuronal subcellular compartments (Jan and Jan, 2012).

Upon translation, Kv channels share the common design of four separate Kvα-subunits, which are assembled in the endoplasmic reticulum (ER) and are subsequently inserted in the plasma membrane (Jan and Jan, 2012). A functionally expressed Kv channel will have six transmembrane domains – denoted S1 through S6 – per Kvα-subunit, which will compose the voltage-sensing and conduction portions of the channel. Kv channels will allow specific passage of potassium ions in response to voltage changes in a cell's membrane potential, playing a crucial role in returning a depolarized cell to resting. Due to their slow opening and slow closing in response to changes in voltage, delayed-rectifier Kv channels are most commonly associated with action potential repolarization.

Delayed-rectifier Kv channels occupy five families – Kv1, Kv2, Kv4, Kv7, and Kv10. Between these families, all members contribute to the descending phase of an action potential by

allowing outward flow of potassium upon membrane depolarization. In a physiological context, delayed-rectifiers limit repetitive firing and action potential duration (Sutherland et al., 1999).

This work will focus exclusively on Kv1 channels.

1.1.2 Kv1 Channel Form and Function

Kv1.1 was first cloned in a mammalian neuron in 1988 (Tempel et al.) following elucidation of the *Drosophila melanogaster* Shaker potassium channel with which it shares high sequence conservation. Mammalian Kv1 channels – Kv1.1., Kv1.2. Kv1.3, Kv1.4 and Kv1.5 – have since been extensively studied, both molecularly and electrophysiologically, and are sometimes referred to as *Shaker*-type voltage-gated potassium channels.

Kv1 channels are homotetrameric at their simplest, but may also be heterotetramers composed of Kvα-subunits from within the Kv1 family (Jan and Jan, 2011), contributing to further functional diversity. The passage of Kv1 channels through open, closed, and inactivated states in response to voltage is often subtype dependent and underlies the waveform of neuronal action potentials. Kv1 channels can attribute the transition between these functional states to discreet domains within their Kvα-subunits (**Figure 1**).

At the protein N-terminal end, the T1 tetramerization domain is involved in proper channel assembly. Consisting of approximately 130 amino acid residues, T1 immediately precedes the first transmembrane domain, S1, on the intracellular side of the membrane (Choe, 2002). A functional domain of T1 in Kv1 channels has an established role of interaction with associated cytoplasmic Kvβ-subunits to modulate channel biophysical properties. In addition, the extreme N-terminal end of Kv1.4 may provide an auto-inhibitory ball, which is used in rapid channel inactivation (Yellen, 2002).

The voltage-sensing region of the channel is located between the first and fourth transmembrane regions (S1-S4) of the individual Kvα-subunits. Specifically, in the fourth transmembrane region, S4, a sequence motif has been identified which is conserved across all types of voltage-gated channels – every third position holds a positively charged lysine or arginine residue (Yellen, 2002). The positively charged residues allow the S4 domain to advance through the neuronal plasma membrane, translocating overall charge of the amino acid sequence while maintaining the charge distribution in the channel core. This may manifest as a stabilized helical screw motion which allows the channel to open in response to changes in voltage in the surrounding membrane (Catterall, 1986).

The S5 and S6 domains contribute to the channel pore, which allows conductance of potassium ions upon opening. Strung between S5 and S6 is the "P Loop" – a conserved amino acid sequence which dips into the membrane without fully crossing it. The four P-loops from each Kvα-subunit in the tetramer will orient together, with the ultimate effect of structurally generating a narrow selectivity filter which allows potassium ions to flow passively through upon opening (Choe, 2002). The selectivity filter is formed by two groups of four carbonyl oxygen atoms every 3 Å within the pore. Potassium ions will interact with these "oxygen cages" in a way that mimics how the ions interact with water molecules (Yellen, 2002), while excluding sodium movement through the pore.

For proper functionality in the context of action potential signalling, Kv1 channels must be expressed in neuronal membranes. The intracellular C-terminal end of the Kvα-subunit has a common PDZ-binding motif, which allows for recognition by signalling complexes and aids in appropriate channel localization in neuronal cells (Yellen, 2002). The PDZ domain is large, with eight segments of secondary structure (Doyle et al. 1996) which will interact specifically with a

known Thr/Ser-X-Val motif on target proteins. Importantly, the PDZ domain interacts postsynaptic density protein 95 (PSD95), aiding in reliability of membrane protein clustering (Doyle et al. 1996).

1.2 Kv1.2 Voltage-Gated Potassium Channels

1.2.1 Structural Determination

Prior to 2005, much of our knowledge of potassium channel structure was based on study of the prokaryotic KcsA and MthK channels. From these channels, it was known that the S6 region of the *Shaker*-type channels corresponds to the KscA "inner helix". The initial understanding of Kv channel gating was further aided by structural determination of the MthK channel in its open state (Zadek and Nimigean, 2006). The structural similarity allowed study of potassium channel conductance at a rudimentary level; however, prokaryotic potassium channels lack the complexity which is found in mammalian potassium channels, making them poor models for the study of Kv channels in complex neuronal signalling.

The first mammalian *Shaker*-type channel to be crystallized and structurally solved was Kv1.2 from *Rattus norvegicus* (Long et al., 2005a). Although missing ~37% of the final protein product, the initial crystal structure of Kv1.2 confirmed that position and orientation of the T1 domain and showed that the Kv1.2 pore was similar to that of prokaryotic channels. It was further shown that the S4 domain voltage sensors performed mechanical work through the S4-S5 linker helices, to constrict or dilate the pore-forming S6 inner helices to generate open and closed states (Long et al., 2005b). Kv1.2 was crystallized with the Kvβ2 auxiliary subunit, and this work was

the first to demonstrate the structural relationship between the pore, the T1 domain, and the Kvβ catalytic domain (Long et al., 2005a).

The entirety of the structure of Kv1.2 was solved in 2012 (Chen et al., 2010), including the previously unsolved transmembrane regions of the channel, providing the final structural insights to the functional domains. A focused electric field was identified, which separates the internal and external charges and is responsible for the ability of S4 positively charged residues to control channel gating in response to changes in membrane voltage. These findings gave novel insight to the closed to open transition of Kv1.2, specifically in the context of voltage-sensitivity. Importantly, Kv1.2 remains the only *Shaker*-type channel with a solved crystal structure.

Due to its high-resolution crystal structure, Kv1.2 is a common channel used in the study of conformational changes associated with Kv channel activation (Horne et al., 2010; Ishida et al., 2015). Interactions between the residues of the highly-conserved voltage-sensing domain are critical for channel activation gating (Liman et al., 1991); however, other regions within the channel can modulate the tine course and voltage-dependency of activation. Typically, other channel regions are less highly-conserved than the voltage-sensing domain, and in this way heterogeneity of activation-gating within the Kv1 channel family is introduced. For example, it has been shown that genetic deletion of the N- or C- terminus of Kv1 channels may drastically shift voltage-dependency of activation (Van Donagen et al., 1990; Cushman et al., 2000), indicating that there are structures outside the voltage-sensing domain and channel pore which are important for channel opening. Kv1 activation gating is of particular importance, as its voltage-dependency influences the threshold for action potential firing within the axon initial segment (Rasbad, 2010).

1.2.2 Kv1.2 Heterogenous Activation Gating

It was first noted that heterotetrameric Kv1 channels lacking Kv1.2 subunits activated at abnormally negative potentials by Brew et al. (2007) with their generation of $KCNA2^{-/-}$ mice. This group postulated that Kv1 channel voltage-dependency of activation was determined by how many Kv1.2 subunits were contained within Kv1 channel complexes, and that neurons may adjust their excitability threshold by adjusting their Kv1.1: Kv1.2 balance. In this way, the presence of Kv1.2 subunits increases the membrane voltage required for channel activation. Interestingly, Kv1.2-null mice show complete mortality within weeks of birth, which contrasts with genetic deletion of other Kv1 channels, which have milder consequences (Smart et al., 1998; Xu et al., 2003; Robbins and Tempel, 2012). Taken together, this evidence hints that Kv1.2 control of activation gating has a distinct and vital role in maintaining appropriate neuronal excitability.

These findings may be explained by a unique property of Kv1.2 within the Kv1 channel family: Kv1.2 displays two distinct modes of activation gating. Recombinant cells expressing Kv1.2 may show "fast" or "slow" activation in response to a depolarizing voltage, manifested as differences in activation kinetics and voltage-dependency of activation (Rezazadeh et al., 2007). "Fast" cells are associated with accelerated activation kinetics and a more negative voltage-dependency of activation, and "slow" cells exhibit slower activation kinetics and a more positive voltage-dependency of activation. This property of Kv1.2 does not represent differences in the channel open state, but rather the opening of channels to a single open state along "fast" and "slow" activation pathways (Rezazadeh et al., 2007).

When a depolarizing prepulse is given in voltage-clamp recordings on cells recombinantly expressing Kv1.2, "slow" cells will shift to "fast" activation gating behaviour. To this end, Kv1.2 channel activation gating mode may be switched from "slow" to "fast", in a phenomenon which

has been termed “prepulse potentiation” or “use-dependent activation” (Grissmer et al., 1994; Baronas et al., 2015). Kv1.2 channels are unique in their ability to generate use-dependent activation, yet they will confer this property to heteromeric Kv1.2-containing Kv1 channel complexes (Brew et al., 2007; Baronas et al. 2015). Use-dependent activation functions to increase neuronal firing threshold potential or terminate bursts of action potentials (Baronas et al., 2015; Grissmer et al., 1994), thus protecting cells from hyperexcitability (Dodson et al., 2003).

A few lines of evidence indicate that a cytoplasmic extrinsic regulator may bind to Kv1.2 in the closed state to regulate activation gating and use-dependent activation. “Slow” activation gating and use-dependence of activation dissipates over time when performing whole-cell recordings, but not when performing perforated patch recordings (Rezazadeh et al., 2007). This observation suggests that a Kv1.2 regulator may be diffusing out of the cell and into the patch pipette during whole cell recordings, such that the perforated patch technique will prevent cytoplasmic diffusion. Further, activation gating shows variability between cell lines recombinantly expressing Kv1.2 (Rezazadeh et al., 2007), suggesting that a factor beyond the primary KCNA2 DNA sequence is required for use-dependence. It has been proposed that a cytoplasmic extrinsic regulator, once referred to as the “soluble gating regulator” (SGR), binds to Kv1.2 in the closed state (Baronas et al., 2016) to regulate Kv1.2 activation gating.

Although the associated signalling molecules have not yet been identified, it is known that an intracellular threonine residue (Thr252) in the S2-S3 linker (**Figure 1**) is responsible for “slow” gating behaviour (Rezazadeh et al., 2007). Modelling studies show that upon depolarization, binding affinity for the SGR in this region is lost, and channels will become “fast’, or disinhibited (Baronas et al., 2016). To this end, “slow” cells with switch to “fast”, but “fast” cells will only stay “fast” in response to a depolarizing prepulse: “fast” activation gating is an indication that the SGR

is not bound to Kv1.2. Identification of the SGR of Kv1.2 will allow for an enhanced understanding of the role of Kv1.2 as a protective channel against hyperexcitability and may give insight into the observed lethality in KNCA2$^{-/-}$ mice.

1.2.3 Mechanisms of Kv1.2 Regulation

Beyond the unidentified SGR which is known to modulate Kv1.2 activation gating, Kv1.2 has been shown to be regulated by glycosylation (Watanabe et al., 2007), phosphorylation (Hattan et al., 2002), N-linked glycans (Zhu et al., 2009), and Src-family protein tyrosine kinases (Nitabach et al., 2000). As Kv1 channels often co-assemble as heterotetramers, the identified regulatory mechanisms of Kv1.2 may also be applied to the other Kv1 channels. In this way, heterogenous assembly in the Kv1 family adds additional layers of control and plasticity, and combinations of Kv1 subtypes may harness unique regulatory pathways (Nitabach et al., 2000; Baronas et al., 2015). It has also been suggested that regulation of Kv1 channels is important at the level of transcription. Overexpression of Kv1 channels within the CNS causes network disruptions and hyperexcitability, indicating a crucial role for gene dosage (Sutherland et al., 1999)

Regulatory mechanisms of Kv1.2 channels often impact evoked action potentials and protein trafficking in addition to channel gating. For instance, glycosylation of Kv1.2 negatively shifts voltage-dependency of activation, affecting action potential properties in simulations (Watanabe et al., 2007). Further, decreasing the glycosylation state of Kv1.2 can increase channel retention in the endoplasmic reticulum (ER), leading to an overall decrease in Kv1.2 cell surface expression. Kv1.2 surface expression may also be affected by the presence of an N-glycan group on the S1-S2 linker, which allows for fidelity of protein folding and trafficking (Zhu et al., 2009). Importantly, the localization of Kv1.2 channels may determine the properties cellular excitability and signalling. It has been shown that presynaptic Kv1.2 channels suppress synaptic terminal

hyperexcitability (Dodson et al., 2003), Kv1.2 in the axon initial segment determines action potential firing threshold (Rasbad, 2010), and Kv1.2 in central synapses modulates inhibitory transmission (Southan and Robertson, 1998).

Kv1.2 channel properties may also be influenced via association with regulatory Kvβ-subunits. Kvβ-subunits are auxiliary subunits specific to the Kv1 family and have important roles in modulating Kv1 channel activity in response to both intra and extracellular signalling cues (Pongs & Schwarz, 2010). Mammalian genomes have three genes which code for Kvβ-subunits: KCNAB1 (Kvβ1), KCNAB2 (Kvβ2), and KCNAB3 (Kvβ3) (Schultz et al., 1996).

1.3 Kvβ Regulatory Subunits

1.3.1 Interaction with Kv1 α-Subunits

Kvβ-subunits have a defined site of interaction with the T_1 domain of the Kvα-subunit. There is a conserved contact loop with complementary amino acid sequences which allows docking of the Kvβ-subunit to the Kvα-subunit with high specificity (Sewing et al., 1996). It has been postulated that Kvα and Kvβ will interact as pre-formed tetramers (Pongs & Schwarz, 2010), which are assembled in the ER and are subsequently trafficked as a whole to the plasma membrane.

The core genetic sequence of the three Kvβ-subunits, coding for approximately 300 amino acids, is highly conserved (Sewing et al., 1996, Accili et al., 1997). Most of the variation between the genes lies in the portion which codes for the N-terminal end, which confers the functional differences between the channel subtypes (Heinemann et al., 1996). Beyond the sequence variation between the Kvβ subtypes, splice variations create additional protein products from the three genes (Wang et al., 1996). Studies of Kv1 channels in rat brain have shown that expression of Kvβ-

subunits can alter Kv1 channel activity by causing rapid inactivation in channels which otherwise do no inactivate (Rettig et al., 1994), via open channel block of the Kv1 pore by the Kvβ N-terminus (Accili et al., 1997).

1.3.2 Function of Kvβ Subunits

Kvβ-subunits allow Kv1 channels to extend much further into to cytoplasm, approximately 100 Å, providing an ideal location for docking of regulatory proteins (Pongs and Schwarz, 2010). Interactors of Kvβ-subunits may include kinases, phosphatases, and other components of signalling pathways. Further, Kvβ-subunits have putative oxidoreductase activity and a NADPH binding pocket (Peri et al., 2001), increasing the complexity of their regulatory activity and adding layers of modulation to overall functionality of Kv1 channels.

In recombinant expression systems, it has been demonstrated that co-expression of Kvα-subunits with Kvβ1 or Kvβ3 can facilitate rapid channel inactivation (Rettig et al., 1994; Heinemann et al., 1996; Pongs and Schwarz, 2010). Kv1 inactivation is important in regulating repetitive electrical activity (Choe, 2002), thus expression of Kvβ-subunits putatively represents a protective measure against hyperexcitability. In contrast, co-expression of Kvβ2 with Kvα-subunits in recombinant systems does not confer altered inactivation properties (Heinemann et al., 1996), due to structural differences in the N-terminus. Rather, expression of Kvβ2 negatively shifts the voltage-dependency of Kv1 channel activation and has been shown to increase Kv1 cell surface expression (Accili et al., 2004). Although Kvβ2 does not have a role in Kv1 channel inactivation, it has shown to be physiologically important, as Kvβ2 null mice exhibit seizures and reduced lifespan (Connor et al., 2005). It is of interest to note that, in theory, any combination of Kvα and Kvβ-subunits may combine, and a nearly infinite number of structurally and functionally distinct Kv1 channels could be created (Sewing et al., 1996)

Another regulator of Kv1 channels has been postulated to behave as a Kvβ-subunit upon ligand-activation (Aydar et al., 2002). This protein, the Sigma-1 Receptor, has no sequence homology to the Kvβ-subunits, but has been shown to decrease Kv1 channel current amplitude and facilitate channel inactivation.

1.4 The Sigma-1 Receptor

1.4.1 Discovery and Classification

The Sigma-1 Receptor (Sig-1R) derives its name from its initial misclassification as an opioid receptor. In the 1960s and 1970s, opioid receptors were divided into four classes based on ligand-binding properties, leading to the naming of μ-receptors, δ-receptors, κ-receptors, and σ-receptors (Sig-1R) (Brownstein, 1993). Early studies of the pharmacology of these receptors showed that μ-receptors, δ-receptors, and κ-receptors were closely related, while Sig-1R remained distinct. The molecular cloning of Sig-1R (Hanner et al., 1996) proved definitively that Sig-1R is dissimilar in sequence from the opioid receptors, and further, Sig-1R has no known sequence homology to any other human protein.

Sig-1R shows high levels of expression in the brain and spinal cord (Weissman et al., 1988; Jansen et al., 1991), and as such has been implicated in the pathophysiology of many psychiatric and neurodegenerative disorders (Matsumoto et al., 2007). Many of its functional roles remain enigmatic, but it is known that Sig-1R resides in the endoplasmic reticulum (ER) and may translocate to other cellular compartments upon ligand activation. Specifically, Sig-1R is enriched at the ER mitochondrion-associated membrane (MAM; Mavlyutov and Ruoho, 2007) to modulate ER-mitochondrion signaling, but is also known to be associated with the nuclear envelope

(Hayashi and Su. 2003), lipid rafts (Hayashi and Su, 2004), and ion channels within the plasma membrane upon ligand-activation (Zhang and Cuevas, 2002; Crottes et al., 2011; Gao et al., 2012). Sig-1R binds promiscuously to a variety of psychotropic drugs, such as ketamine, haloperidol, pentazocine, and cocaine (Maurice and Su, 2009), and pharmacological activation triggers its regulatory roles as an inter-organelle signalling modulator (Su et al., 2010).

1.4.2 Crystallization and Structural Insights

Prior to 2016, remarkably little information was known about the structure of Sig-1R and its function at the molecular level. Recent Sig-1R crystallization revealed that the receptor exists in a homotrimeric structure in the ligand-bound state (Schmidt et al., 2016). Each monomer of Sig-1R contains a single N-terminal transmembrane domain, which crosses from the luminal side of the ER to cytoplasm (Mavylutov et al., 2017). The C-terminal domain of Sig-1R associates with the ER membrane and forms a flat, hydrophobic surface. The crystal structure further revealed a β-barrrel which holds the ligand-binding domain, which exists as a large and hydrophobic cavity and shows great variability in its capacity for ligand recognition (Schmidt et al., 2016).

Antibody accessibility techniques were initially used to determine the topology of Sig-1R prior to crystallization, with mixed findings. A first report found that both N- and C-termini faced the cytosol (Aydar et al., 2002), and a later report found that both the N- and C- termini were facing the ER lumen (Hayashi and Su, 2007). Enhanced resolution Electron Microscopy (EM) claimed to indisputably resolve Sig-1R topology with the finding that the bulk of the protein is within the ER-lumen (Mavylutov et al., 2017). Although experimentally meticulous, the ER-luminal facing topology of Sig-1R is counterintuitive to its known functional properties, specifically in terms of modulation of plasma membrane-resident ion channels. To explain these findings, it was suggested that the interaction of Sig-1R with plasma membrane ion channels is due to the role of Sig-1R and

the ER in subcellular sorting prior to trafficking of proteins to their final destination (Mavylutov et al., 2017), but this account is not entirely pleasing. To this end, Sig-1R topology is still poorly understood, and more studies are required to elucidate the overall protein architecture.

1.4.3 Sig-1R Modulation of Neuronal Excitability

It has been noted that the most prominent action of Sig-1R is the regulation ion channels (Maurice and Su, 2009). Sig-1R has been shown to modulate calcium, potassium, sodium, and chloride channels, in addition to SK channels, NMDA receptors and IP3 receptors. The defined interaction of Sig-1R with ion channels is known to influence neuronal plasticity (Kourrich et al., 2013) and intrinsic neuronal excitability.

Excitatory transmission in the CNS and in the PNS may be regulated by Sig-1R via varied cellular mechanisms involving ligand-gated channels (Bergeron et al., 1993; Yoon et al., 2003). For instance, Sig-1R has been implicated in NMDAR-mediated transmission and is involved in excitatory glutamatergic transmission via both pre and postsynaptic receptors. Sig-1R activation can trigger an intracellular mechanism allowing presynaptic glutamate release, but can also suppress NMDAR-mediated evoked EPSCs, depending on the subcellular site of action (Kourrich, 2017). Ultimately, these Sig-1R dependent modulations within the synapse will alter the neuronal capacity to generate an EPSP.

Additionally, Sig-1R has many defined regulatory mechanisms of channels which conduct and propagate the action potential following its initial generation at the synapse. Pharmacological activation of Sig-1R has been proven to regulate various voltage-gated ion channels, including Nav and Kv channels. In fact, Sig-1R meets all the criteria as an atypical auxiliary subunit for the ion channels which underlie propagation of neuronal signaling (Kourrich, 2017). Auxiliary

subunits are non-conducting components of ion channels which have the capability to directly modulate the biophysical properties of the pore-forming α-subunits, aid in assembly and trafficking of the pore-forming α-subunits to the plasma membrane, and alter pharmacological interactions with the channel (Kourrich, 2017). The role of Sig-1R as a ligand-regulated auxiliary subunit is particularly notable in the Kv1 voltage-gated potassium channel family.

1.4.4 Sig-1R Modulation of Kv1 Channels

The body of work which defines the interaction of Sig-1R with Kv1 channels is small but robust. Although the members of the Kv1 family are highly homologous, differences in the primary amino acid sequences exist between the members. As such, differences in Sig-1R modulation of Kv1 channel members has been noted. Voltage-clamp recordings of *Xenopus* oocytes recombinantly expressing either Kv1.4 or Kv1.5 revealed that application of the Sig-1R agonist SKF-10,047 (SKF) decreased channel current amplitude. SKF application was also shown to accelerate Kv1.4 channel inactivation (Aydar et al., 2002), and co-immunoprecipitation (Co-IP) of Kv1.4 and Sig-1R suggest that these effects are due to a direct interaction.

Another member of the Kv1 family, Kv1.3, was additionally shown to directly interact with Sig-1R, but application of each of the Sig-1R ligands SKF, ketamine, and haloperidol resulted in no change in Kv1.3 current amplitude in voltage-clamp recordings of *Xenopus* oocytes (Kourrich et al., 2012). However, it was found that co-expression of Sig-1R with Kv1.3 was sufficient to accelerate Kv1.3 inactivation kinetics.

Sig-1R regulation of Kv1 channels has also shown to be dynamic: acute application of Sig-1R agonists may decrease potassium conductance through Kv1 channels (Aydar et al., 2002), but chronic treatment promotes Kv1.2 channel trafficking to the plasma membrane (Kourrich et al.,

2012). Although several mechanisms of regulation have been identified in recombinant systems, Sig-1R modulation of Kv1 channels is still largely uncharacterized.

As per these findings, it has been postulated that Sig-1R interacts with Kv1 channels as an auxiliary subunit (Aydar et al., 2002), similarly to the Kvβ-subunits. Sig-1R has been shown to modulate Kv1 biophysical properties, facilitate trafficking to the plasma membrane, and bind ligands directly to modulate channel activity, which meets the criteria of an auxiliary subunit. However, Sig-1R regulation of Kvα-subunits bears some significant differences from Kvβ regulation of Kvα-1subunits. Firstly, Sig-1R interacts with a Kv1.3 transmembrane domain (Kinoshita et al., 2012), whilst Kvβ-subunits exert their inactivation effects via a well-characterized interaction with the Kv1 N-terminal T1 domain (Rettig et al. 1994). Secondly, Sig-1R modulates a multitude of ion channels to control neuronal excitability, whilst Kvβ-subunits are specific to Kv1 channels. Finally, Sig-1R regulation of Kv1 channels appears to be dynamic, whilst Kvβ-subunits reliably exert predictable effects on channel conductance and inactivation. Thus, although Sig-1R and Kvβ-subunits are faithful modulators of Kv1 channels, Sig-1R remains distinct and unique in its mode of action.

Beyond the putative role of Sig-1R as a Kv1-auxiliary subunit, Sig-1R may be a candidate as the yet unidentified SGR, which associates with Kv1.2 to produce “slow” activation gating (Baronas et al., 2016). Biophysical studies of Sig-1R ligand-activation on Kv1.2 channels are notably missing. In *vivo* studies in mice have shown that chronic treatment with cocaine causes a Sig-1R dependent upregulation of Kv1.2 in the nucleus accumbens (Kourrich et al., 2012), but it is yet unknown if this is paired with changes in Kv1.2 channel activation, inactivation, or ion conductance. As Kv1.2 is associated Kv1 channel plasticity via heterogenous activation gating and modulation by extrinsic regulators, the biophysical consequences of Sig-1R association with Kv1.2

will enhance our understanding of Sig-1R control of action potential propagation. Further, identification of Sig-1R as the SGR will provide crucial insights to the role of Kv1.2 in limiting repetitive firing and ultimately protecting against hyperexcitability.

1.5 Implications in Motor Neuron Disease

1.5.1 Hyperexcitability and Motor Neurons

The motor neuron diseases (MND) are a group of progressive neurodegenerative disorders which selectively affect upper and lower motor neurons. MNDs can be sporadic or hereditary and have varied symptoms including spasms, cramps, fasciculations, weakness, spasticity (stiffness), and loss of voluntary muscular control. Diseases in this family are classified by the cell type affected – upper motor neurons, lower motor neurons, or both – and include amyotrophic lateral sclerosis (ALS), hereditary spastic paraplegia (HSP), progressive muscular atrophy (PMA), and various other motor neuropathies. On a cellular level, excitotoxicity is thought to play a role in the selective death of motor neurons in MND (Shaw, 1994).

Excitotoxicity in neurodegeneration was a term coined to describe excessive glutamatergic synapse activity (Olney, 1978), which leads to neuronal hyperexcitability and toxic elevation of intracellular calcium (Pasinelli and Brown, 2006). Primary excitotoxicity may be a result of increased availability of glutamate in excitatory synapses or increased amounts of glutamate-mediated cation channels in motor neurons; however, excitotoxicity may occur as a secondary mechanism, which is symptomatic of other dysfunctional cellular processes, such that neuronal energy metabolism is disrupted, membrane resting potential is altered, and NMDARs may be overactivated by normal glutamate levels in the synapse (Shaw, 1994). No matter the source of

excitotoxicity, the observed increase of free calcium within motor neurons is upstream of ER stress pathways, which may trigger the Unfolded Protein Response (UPR) leading to cell death cascades (Kiskinis et al., 2014).

Although excitotoxicity refers to increased glutamate in excitatory synapses, alteration in activity and expression of delayed-rectifier potassium channels has also been associated with toxic hyperexcitability in individuals with MND. Beyond the synapse, hyperexcitability in axons has been noted in MND patients (Nakata et al., 2006), suggesting a mechanism which likely involves decreased activity of delayed-rectifier potassium channels (Kanai et al., 2006). The degree of hyperexcitability in axons of motor neurons is known to correlate with patient survival (Kanai et al., 2012), but if this hyperexcitability is due to primary or secondary mechanisms has yet to be elucidated. Thus, the investigation of the role of Kv channels in MND may provide valuable insights to disease pathogenesis.

It has been observed that delayed-rectifier potassium channel current is reduced in a broad group of ALS patient motor neurons derived from iPSCs (Wainger et al., 2014). Similarly, there are reduced levels of Kv1.2 in patients with sporadic ALS, as determined by post-mortem immunohistochemistry (Shibuya et al., 2011). These lines of evidence point to a specific role for Kv1.2 in the protection against hyperexcitability in MND. Overall, hyperexcitability has been implicated in MND pathogenesis, and Kv1.2 has been implicated in hyperexcitability. For instance, Kv1.2 has a known role in the presynaptic membrane to suppress terminal hyperexcitability in response to trains of action potentials (Dodson et al., 2003).

1.5.2 Consequences of KCNA2 and SIGMAR1 Mutation

Although Kv1.2 gain of function (GOF) is often associated with epilepsy (Robbins and Tempel, 2012; Syrbe et al., 2015; Pena and Coimbra, 2015), Kv1.2 has also been linked with the pathophysiology of other disorders, including MND. Specifically, a recurrent mutation in the KCNA2 gene was recently identified in two unrelated families, which resulted in HSP (Helbig et al., 2016). This mutation was classified as a missense mutation in the gene region coding for the Kv1.2 S4 voltage-sensor domain, and results in loss of function (LOF) in voltage-clamp recordings of recombinant *Xenopus* oocytes. These findings reaffirm that decreased delayed-rectifier potassium current in motor neurons may mediate MND, and Kv1.2 – with its unique ability to display bimodal activation gating – may be disproportionately important in protecting against motor neuron hyperexcitability.

Gene mutations in SIGMAR1 have also shown to result in MND. An in-frame deletion of 60 base pairs within the first exon of Sig-1R was identified in a consanguineous Chinese family (Li et al., 2015), which results in distal hereditary motor neuropathy (dHMN). This mutation generates a Sig-1R which lacks the α2 helix encoded by amino acids 31-50. Characterization of this Sig-1R mutant in recombinant mammalian cell lines revealed aberrant subcellular dynamics as compared to the WT Sig-1R, with diffuse/ cytosolic localization and increased mobility (Wong et al., 2016), likely due to gross structural changes and impaired protein assembly.

The involvement of Sig-1R in MND is further emphasized by the identification of another recurrent mutation in the SIGMAR1 gene, which results in ALS16 (Al-Saif et al., 2011). ALS16 is a severe form of juvenile ALS and has been attributed to a single missense mutation in SIGMAR1, causing the substitution of glutamine for glutamic acid at position 102 (E102Q). Sig-1R-E102Q has been extensively characterized, revealing mitochondrial dysfunction (Fukunaga et

al., 2015), ER-stress mediated disruptions in protein homeostasis (Dreser et al., 2017) and upregulation of inwardly-rectifying potassium channel current (Wong et al., 2016).

It is important to note that Sig-1R is expressed in all tissue types, but SIGMAR1 mutations exclusively result in MND phenotypes. To this end, we speculate that the pathophysiology associated with SIGMAR1 mutations is mediated by dysfunctional interaction and regulation of proteins which are specifically important in motor neuron function. Given that Sig-1R is a known modulator of Kv1 channels and has further been shown to co-immunoprecipitate with Kv1.2, we predict that the neurodegeneration observed in individuals with SIGMAR1 mutations is due to a dysfunctional modulatory interaction of Sig-1R and Kv1.2.

Based on all lines of evidence, we predict that dysfunctional modulation of Kv1.2 by Sig-1R may represent a hitherto uncharacterized mechanism of hyperexcitability in motor neurons, leading to MND phenotypes when there are mutations within gene coding for Sig-1R. To this end, this thesis of work will begin by characterizing the interaction of Kv1.2 and Sig-1R, then will examine the implications of this interaction when the mutant Sig-1R underlying ALS16 is expressed.

HYPOTHESIS:

The Sigma-1 Receptor regulates Kv1.2 voltage-gated potassium channel activation gating, current amplitude, and inactivation as an auxiliary subunit upon ligand-activation, and this regulation is altered when the mutant Sigma-1 Receptor underlying ALS16 is expressed.

Specific Aims:

Aim 1: apFRET imaging of the interaction between Sig-1R and Kv1.2

Aim 2: Electrophysiological characterization of Kv1.2 in response to Sig-1R ligand-activation

Aim 3: Sig-1R as a Kv1.2 regulatory ancillary subunit

Aim 4: Implications of Sig-1R modulation of Kv1.2 in ALS16

2. MATERIALS AND METHODS

2.1 Cell culture and cDNA transfection

All experiments were performed on HEK293 cells grown in Dulbecco's modified Eagle medium (DMEM: Wisent Inc.), containing 10% fetal bovine serum (FBS), 100 U/mL penicillin/streptomycin and 1X GlutaMAX (Gibco/Invitrogen) in a humidified 37^{o}C, 5% CO_2 incubator. Cells were washed with phosphate buffered saline (PBS: 10 mM Na_2HPO_4, 1.76 mM KH_2PO_4, 137 mM NaCl, and 2.68 mM KCl; pH 7.2) and passaged upon reaching 80% confluence (roughly every 3-4 days) using trypsination (0.05% trypsin; Gibco/Invitrogen). For live-cell imaging and electrophysiology experiments, cells were respectively plated on 35 mm µ-Dishes (ibidi GmbH, Martinsreid, Germany) and 15 mm Thermanox (Thermo Fisher Scientific) plastic coverslips at a density of 02.x10^6 cells/mL. The day following plating, cells were transiently transfected using TransIT-2020 transfection reagent (Mirus Bio) per manufacturer protocol. A list of constructs used in this work may be found in **Table 1**.

2.2 Voltage-clamp electrophysiology

Whole-cell voltage-clamp recordings were performed on HEK293 cells transiently expressing Kv1.2 and eYFP or Sig-1R-YFP. Cells were imaged under epifluorescence, and only cells displaying YFP fluorescence were selected for recordings. HEK293 cells were held at a membrane potential of -60 mV and were depolarized to membrane voltages between -40 and 80 mV, for 1 – 5 s duration, with 40 s intersweep interval. Cells were found to be stable up to 1 hour. Data was analyzed using Clampfit (Molecular Devices, Sunnyvale, CA), to determine current amplitude in response to voltage steps. Whole-cell current was leak-subtracted prior to analysis.

Potassium conductance (G) was calculated from peak current, according to Hodgkin and Huxley (1952b):

$$G_{K^+} = \frac{I_{K^+}}{\left(V_m - \left(\frac{RT}{F} \ln \frac{[K^+]_{out}}{[K^+]_{in}}\right)\right)}$$

where G_{K+} (G) is potassium conductance, I_{K+} is the potassium current peak, V_m is the membrane voltage, R is the universal gas constant, T is temperature (in Kelvin), F is the Faraday constant, and $[K^+]_{out}$ and $[K^+]_{in}$ are the potassium ion concentrations outside and inside the cells, respectively. For each voltage step, G was normalized G_{max}, and values were plotted to generate voltage-dependency of activation plots.

Voltage-dependency plots were fit with a single Boltzmann sigmoidal (two-state model) to derive $V_{1/2}$, using the formula:

$$P_{open} = \frac{1}{1 + exp\left(\frac{v_{m-V_{1/2}}}{k}\right)}$$

where $V_{1/2}$ describes the voltage at which P_{open} = 0.5, V_m is the membrane voltage, and k is the slope factor, in mV.

2.3 Solutions

All electrophysiological experiments were performed with cells in an external bath solution containing 150 mM NaCl, 10 mM HEPES, 3 mM KCl, 10 mM MgSO4, 2 mM CaCl2, and 10 mM Na-ascorbate, adjusted to pH 7.4 with NaOH, with a flow rate for application of ~1 mL/min. Thick-walled borosilicate glass electrodes (1.5 mm OD, 0.9 mm ID) were filled with an internal K+-Gluconate solution containing 115 mM K+-Glu, 20 mM KCl, 10 mM HEPES, 4 mM Mg2+-ATP, 0.5 mM GTP, and 10 mM Na-Phosphocreatine. Internal solution pH was adjusted to 7.4 using 5

N KOH. Osmolarity of both solutions was adjusted to 290 mOsm using sucrose. E_{rev} was determined to be -80 mV using the Nernst equation.

2.4 FRET Microscopy

FRET experiments were performed on HEK293 cells expressing equimolar amounts of Sig-1R-mCh and Kv1.2-GFP using a Zeiss LSM880 AxioObserverZ1 Confocal Microscope, with excitation wavelengths of 561 nm and 488 nm for mCh and GFP respectively. Cells were imaged in Phenol Red free MEM (Wisent) containing 10% FBS on a pre-warmed 37 ^{0}C stage with 5% CO_2, using a 63× (NA 1.4) oil immersion objective (Zeiss). A resolution of 512 x 512 pixels was used, with a dwell time of 0.5 μsec/ pixel. Following 5 frames of prebleach baseline, a square Region of Interest (ROI) was bleached at 80% 561 nm laser power for 2.5 s. 15 frames were captured postbleach. FRET efficiency was measured via increased donor (GFP) emission following acceptor photobleaching (mCh), using the formula:

$$E = 1- (I_{pre} / I_{post})$$

where I_{pre} and I_{post} are the fluorescent intensities of the donor before and after photobleaching (Bajar et al., 2016). Mean fluorescent intensities within the ROI were determined using Fiji (ImageJ) and were background subtracted prior to analysis. As an internal control, FRET efficiency was calculated within a nonbleached ROI of each cell to account for false-positive FRET signals.

2.5 Western blotting

HEK293 cellss were plated and allowed to grow. 24 h following transfection with construct of interest, cells were lysed on ice with 500 μL radioimmunoprecipitation buffer (RIPA: 150 mM

NaCl, 50 mM Tris, 0.5% sodium deoxycholate, 0.1% NP-40, 5 mM sodium pyrophosphate, 2 mM β-glycerophosphate, 1×EDTA-free protease inhibitor (Fisher Scientific), pH 7.5), and total protein concentration was determined with DC protein assay. Total protein (1.5 mg per lane) was resolved on Tris-glycine SDS-PAGE and transferred onto PVDF membrane. After incubation with primary and secondary antibodies dissolved in 5% milk, membranes were developed using Luminata Forte (Millipore, Darmstadt, Germany) and visualized using LI-COR Odyssey Fc (LI-COR, Lincoln, Nebraska USA). Band intensities were normalized to total protein as determined by Fast Green stain (125 μM Fast Green FCF (Sigma-Aldrich, Oakville, ON, Canada), 6.7% acetic acid, 30% methanol).

2.6 Drugs and Antibodies

The Sig-1R agonist (2S,6S,11S)-1,2,3,4,5,6-Hexahydro-6,11-dimethyl-3-(2-propenyl)-2,6-methano-3-benzazocin-8- ol hydrochloride (SKF 10,047; SKF) was obtained from Tocris (Ellisville, MO). SKF was dissolved in ddH_2O to a stock concentration of 50 mM, and was added to cell bath solutions to achieve a final concentration of 50 μM in all cases.

The following antibodies and dilutions were used for Western blotting: Rabbit-polyclonal anti-KCNAB2 (1:500; OriGene Technologies) and HRP-conjugated rabbit secondary antibody (1:15000; Jackson ImmunoResearch).

2.7 Analysis and Statistics

Prism 7 (GraphPad) was used for graph design, statistics, and curve fitting. Unless otherwise stated, all data is presented as mean ± SEM. Statistical significance was determined

using ANOVA for multiple comparisons or an unpaired Student's t-test for comparison of independent groups. Data was considered significant if $p < 0.05$.

3. RESULTS

The results section is organized into four aims:

Aim 1: apFRET imaging of the interaction between Sig-1R and Kv1.2

Aim 2: Electrophysiological characterization of Kv1.2 in response to Sig-1R ligand-activation

Aim 3: Sig-1R as a Kv1.2 regulatory ancillary subunit

Aim 4: Implications of Sig-1R modulation of Kv1.2 in ALS16

3.1 Aim 1: apFRET imaging of the interaction between Kv1.2 and Sig-1R

3.1.1 Sig-1R directly interacts with Kv1.2 in live cells

Previous studies provide strong indirect evidence of an interaction between Sig-1R and *Shaker*-type voltage-gated potassium channels (Kv1.x channels) and demonstrate that Sig-1R agonist application facilitates increased interaction between these proteins (Kourrich et al., 2013; Delint-Ramirez et al., 2018). Results from co-immunoprecipitation (co-IP) experiments show that Sig-1R interacts with Kv1.3 and Kv1.4 in *Xenopus* recombinant systems (Aydar et al., 2002; Kinoshita et al., 2012), and with Kv1.2 in mouse prefrontal cortex and nucleus accumbens (Kourrich et al., 2013; Delint-Ramirez et al., 2018). We sought to build upon these findings and determine if Sig-1R and Kv1.2 can directly interact in a recombinant system. To this end, we transfected HEK293 cells with Sig-1R-mCh and Kv1.2-GFP and performed acceptor-photobleaching Fluorescence Resonance Energy Transfer (apFRET) in the presence and absence of the Sig-1R agonist SKF-10,047 (50 μM: Tocris; Zukin et al., 1988).

apFRET is dependent on emission energy transfer from the co-expressed fluorescent donor to the acceptor, such that excitation of the acceptor will quench donor emission when the proteins are in close proximity (Bajar et al., 2016; Martin et al., 2018). FRET efficiency is

measured using the change in donor fluorophore emission intensity (GFP intensity) following bleaching of the acceptor fluorophore (mCh). Thus, an increase in GFP intensity indicates de-quenching, and FRET efficiency may be calculated such that a FRET efficiency of 50% designates a Förster distance of ≤ 5.4 nm between the proteins of interest (**Figure 2;** Lam et al., 2012; Bajar et al., 2016). Kv1.2-GFP was used as the donor fluorophore and Sig-1R-mCh was used as the acceptor fluorophore. FRET efficiency calculations were performed by measuring mean GFP intensity per frame before and after mCh bleaching (**Figure 3A-B**). A control (non-bleached) ROI was used to control for false-positive FRET efficiencies in each cell (Organ-Darling et al., 2013).

Prior to SKF treatment, FRET efficiency was found to be 21.8 ± 0.96% in the bleached ROI, versus 0.82 ± 0.81% in the control region (**Figure 3C**). One-way ANOVA determined a significant effect of acceptor photobleaching on FRET efficiency ($n = 29$; $p < 0.0001$). These results confirm the finding that Kv1.2 and Sig-1R are interacting in baseline conditions (Kourrich et al., 2013). When HEK293 cells were acutely treated with SKF, FRET efficiency was determined to be 21.4 ± 1.42% in the bleached ROI versus 0.15 ± 0.79% in the control ROI ($n = 21$; $p < 0.0001$). FRET efficiency was compared in the bleached ROIs between cells at baseline ($n = 29$) and cells treated with SKF ($n = 21$), and it was found that there was no significant difference between these groups ($p = 0.99$). Further, treated cells and untreated cells showed similar Fluorescence Recovery After Photobleaching (FRAP: **Figure 3D**) of Sig-1R-mCh, indicating that Sig-1R had similar mobility in both groups ($p = 0.8442$).

Therefore, these results demonstrate that Sig-1R is interacting with Kv1.2 in the absence of ligand and application of SKF does not facilitate further interaction.

3.1.2 Prolonged treatment with SKF decreases Sig-1R interaction with Kv1.2

As it is known that repeated Sig-1R agonist exposure increases Sig-1R co-IP with Kv1.2 in *vivo* (Kourrich et al., 2013), we hypothesized that extending the duration of SKF treatment may facilitate increased recruitment of Sig-1R to Kv1.2 in our experimental system. To this end, we repeated our apFRET imaging paradigm with cells that were treated with SKF 18 h prior to imaging (**Figure 4A**).

FRET efficiency after 18 h SKF treatment was 12.1 ± 0.85% in the bleached ROI and 0.13 ± 0.8% in the control region (Figure 4B; $n = 24$; $p < 0.0001$), demonstrating that Sig-1R is still interacting with Kv1.2. However, when FRET efficiency was compared between cells without SKF treatment ($n = 29$) and cells with 18 h SKF treatment ($n = 24$), there was a significant decrease in FRET efficiency in 18 h SKF treated cells ($p < 0.0001$). Further, the 18 h SKF treated cells exhibited accelerated FRAP of Sig-1R-mCh as compared to untreated cells ($p < 0.0001$; **Figure 4C**), indicating that prolonged SKF treatment increases Sig-1R mobility, as previously observed in our laboratory (Wong et al., 2016).

The increased mobility of the ligand-activated Sig-1R may indicate that Sig-1R is moving within its subcellular compartments to interact with various proteins (Hayashi and Su. 2007). Beyond increased mobility, we show novel results that extended treatment with SKF decreases Sig-1R interaction with Kv1.2. Although the underlying mechanism remains unclear, these findings indicate that modulation of Kv1.2 via a direct interaction with Sig-1R is dependent on the duration of ligand application: when Sig-1R is in the presence of ligand for a prolonged period, interaction with Kv1.2 is reduced.

3.2 Aim 2: Electrophysiological characterization Kv1.2 in response to Sig-1R ligand-activation

3.2.1 Ligand-activation of Sig-1R decreases Kv1.2 current amplitude

Increasing evidence from electrophysiological studies have shown that the modulation of Kv1 channels by Sig-1R is subtype dependent. Pharmacological activation of Sig-1R decreases Kv1.4 and Kv1.5 current amplitude and accelerates Kv1.4 inactivation kinetics in recombinant *Xenopus* oocytes (Aydar et al. 2002). In contrast, Kv1.3 current amplitude is not affected by treatment with Sig-1R ligands, but co-expression of Sig-1R is sufficient to accelerate Kv1.3 channel inactivation (Kinoshita et al. 2012). It is known that the cocaine, a Sig-1R agonist (Sharkey et al. 1988), promotes trafficking of Kv1.2 to the plasma membrane (Kourrich et al. 2013; Delint-Ramirez et al 2018), but it is unknown how Sig-1R acutely modulates Kv1.2 in recombinant systems. Analogous to what is observed in other Kv1 channels, we hypothesized that SKF application may impact Kv1.2 current amplitude, inactivation kinetics, and voltage-dependency of inactivation.

We used voltage-clamp electrophysiology in HEK293 cells to characterize the effect of Sig-1R ligand-activation on Kv1.2 channels. Each cell was given a 5 s prepulse, ranging from -60 mV to +80 mV (in increments of 20 mV), followed by a 1 s +80 mV test potential step (**Figure 5A**). Peak current amplitude from the prepulse was used to generate current-voltage plots (IV plots). Voltage-dependency of inactivation was determined by subtracting the 5 s steady-state current for each given prepulse voltage from peak current at the + 80 mV test pulse. All values were normalized to +80 mV prepulse peak current. Normalized values were plotted against voltage and fitted with a single Boltzmann function (see methods) to derive $V_{1/2}$ of inactivation. Recordings were performed on cells expressing Kv1.2 and Sig-1R-YFP, and on cells expressing Kv1.2 and

eYFP. As our apFRET experiments were constrained to overexpression due to the need for a fluorescently-tagged Sig-1R, we aimed to verify that cells overexpressing Sig-1R and cells endogenously expressing Sig-1R behaved similarly in response to SKF application.

Upon treatment with SKF, we found that cells expressing Kv1.2 and Sig-1R-YFP displayed a 28.2 ± 2.1% decrease in current amplitude at +80 mV, with significant decreases in current amplitude at all voltages greater than + 20 mV ($n = 10$; $p < 0.0001$; **Figure 5C**), which was not reversed upon drug washout (**Figure 5E**). Similarly, cells expressing Kv1.2 and eYFP showed an irreversible 22.2 ± 2.9% decrease in current amplitude at +80 mV upon application of SKF ($n = 8$; $p < 0.0001$; **Figure 5D**). Comparison of both SKF treated groups revealed no significant differences ($p > 0.05$), and it was determined that overexpression of Sig-1R had no effect on the change in current amplitude in response to SKF treatment.

Characterization of Kv1.2 revealed considerable heterogeneity in terms of kinetics and $V_{1/2}$ of inactivation. To this end, inactivation kinetics and mean $V_{1/2}$ of inactivation are not reported in this thesis as we do not believe they are not representative values. Despite heterogeneity in these parameters, voltage-dependency of inactivation was compared in cells expressing Kv1.2 and Sig-1R-YFP ($n = 10$; **Figure 5F**) and cells expressing Kv1.2 and eYFP ($n = 8$; **Figure 5G**) in response to Sig-1R ligand application. It was found that SKF had no effect on Kv1.2 inactivation in both groups.

Taken together, these results demonstrate that pharmacological activation of Sig-1R acutely modulates Kv1.2 channels. Application of SKF triggers an irreversible decrease in Kv1.2 current amplitude whilst having no impact on Kv1.2 inactivation. These effects are likely due to ligand-dependent changes in Sig-1R activity, and not due to acute Sig-1R recruitment to Kv1.2

channels (**Figure 3**). We speculate that ligand-binding may cause conformational changes in Sig-1R, which in turn lead to changes in receptor and channel functionality.

3.2.2 When Sig-1R is overexpressed, Kv1.2 is more likely to exhibit "slow" activation gating

Unique within the Kv1 channel family, Kv1.2 is known to display heterogenous activation gating (Grissmer et al., 1994; Rezazadeh et al., 2007). Recombinant cells expressing Kv1.2 may show "fast" or "slow" activation in response to a depolarizing voltage, manifested as differences in activation kinetics and voltage-dependency of activation. Although the associated signalling molecules have not yet been identified, it is known that an intracellular threonine residue (Thr252) in the S2-S3 linker of Kv1.2 is responsible for "slow" gating behaviour (Rezazadeh et al., 2007). Thr252 has also been associated with Kv1.2 use-dependent activation (Baronas et al., 2016), which may function to increase neuronal firing threshold potential or terminate bursts of action potentials (Baronas et al., 2015; Grissmer et al., 1994). It has been suggested that a cytoplasmic (Rezazadeh et al., 2007) extrinsic regulator may bind to Kv1.2 in the closed state (Baronas et al., 2016) to regulate activation gating and use-dependent activation.

We sought to confirm that Kv1.2 exhibited bimodal activation gating in response to prepulse conditioning within our experimental system by adapting a protocol used by Rezazadeh et al. (2007). Activation curves were generated by stepping cells from -60 mV to +60 mV (Δ 10 mV) and measuring peak conductance (G). Following a 5 s repolarizing step at -60 mV, cells were then given a + 60 mV prepulse, to induce prepulse potentiation, before repeating the activation protocol (**Figure 6A**). G/G_{max} was calculated and fitted with a single Boltzmann function, for both activation curves, to derive $V_{1/2}$ of activation. In cells exhibiting "slow" gating, the prepulse will induce a leftward shift in $V_{1/2}$ of activation and will accelerate channel activation kinetics. In

contrast, “fast” cells will show no further potentiation in response to the prepulse (**Figure 6B—D**) It has been shown that prepulse dependent acceleration of activation is not caused by incomplete deactivation during the interpulse interval and is instead due to a depolarization dependent shift from “slow” gating to “fast” gating (Rezazdeh et al., 2007; Baronas et al., 2016).

It has been reported that “fast” cells and “slow” cells may differ in $V_{1/2}$ of activation by greater than 30 mV (Baronas et al., 2015; Rezazadeh et al., 2007). However, in our hands $V_{1/2}$ of activation in “fast” and “slow” cells reliably differs by 6—10 mV (**Figure 6**). We found that activation kinetics were a more reliable indication of “fast” versus “slow” cells, with “fast” cells displaying an activation tau of 11.63 ± 0.44 ms at +60 mV and “slow” cells displaying an activation tau of 2.73 ± 0.18 ms at + 60 mV (**Figure 6B**).

We next sought to investigate the effect of Sig-1R ligand-activation on Kv1.2 activation gating mode. Cells expressing Kv1.2 and Sig-1R-YFP showed an activation tau of 1.91 ± 0.13 ms at +60 mV in the “fast” state and 13.71 ± 1.99 ms in the “slow” state (n = 22; **Figure 7C**), with “fast” cells exhibiting a leftward shift in $V_{1/2}$ of activation of ~7 mV (**Figure 7A**). Similarly, cell expressing Kv1.2 and eYFP showed an activation tau of 2.01 ± 0.28 ms at +60 mV in the “fast” state and 11.68 ± 0.66 ms in the “slow” state (n = 18; **Figure 7C**), with a leftward shift of 6 mV in the “fast” $V_{1/2}$ of activation (**Figure 7B**). Interestingly, a group difference between cells expressing Sig-1R-YFP and eYFP was observed. We determined that cells overexpressing Sig-1R were more likely to be “slow”, and cells expressing eYFP were more likely to be “fast” (**Figure 7D**). Despite this, treatment with SKF had no effect on Kv1.2 activation kinetics or voltage-dependency of activation in both cells expressing Sig-1R-YFP and cells expressing eYFP (**Figure 8**).

Here, we show that overexpression of Sig-1R increases the proportion of Kv1.2-expressing cells displaying the "slow" gating mode. In contrast, cells expressing eYFP may have a higher proportion of Kv1.2 channels in the "fast" gating mode, likely due to the stoichiometric difference of Sig-1R to Kv1.2 channels. These results are a new indication that the level of expression of Sig-1R may alter the functionality of Kv1.2 channels.

3.3 Aim 3: Sig-1R as a Kv1.2 regulatory ancillary subunit

3.3.1 Expression of Kvβ2 blocks the effect of Sig-1R ligand-activation on Kv1.2

We next sought to determine if we could occlude the effects of Sig-1R ligand activation on Kv1.2 current amplitude and of Sig-1R overexpression on Kv1.2 activation, via expression of a known Kv1.2 binding partner. Kv1 channels are known to interact with regulatory Kvβ-subunits (Rettig et al., 1994; Heinemann et al., 1996; Nakahira et al., 1996; Accili et al., 1997). KvB-subunits bind to Kv1 channels to modulate channel inactivation and cell surface expression (Shi et al., 1996), via interaction with the channel intracellular T_1 domain (Rettig et al., 1994; Accili et al., 1997). Three subtypes of Kvβ-subunits have been identified and have been characterized for their interaction with Kv1 α-subunits.

We hypothesized that expression of a Kvβ subunit may reduce the effects of SKF on Kv1.2 channel activity. We chose to use Kvβ2, which is a non-inactivating Kvβ-subunit, for electrophysiology experiments. Kvβ1-subunits are the most well-characterized of the Kvβ-subunits, but they typically confer rapid inactivation in Kv1 channels (Heinemann et al., 1996), which may mask the effects of Sig-1R ligand-activation. Kvβ2 has been shown to slightly alter $V_{1/2}$ of activation and activation kinetics in Kv1.5 (Heinemann et al., 1996), but has not been shown to confer rapid inactivation.

We first confirmed that HEK293 cells do not endogenously express Kvβ2, and that transfection with Kvβ2 cDNA would induce Kvβ2 protein expression, via western blotting (**Figure 9A**). Cells expressing Kv1.2, eYFP, and Kvβ2 were characterized in the presence and absence of SKF, as previously described. The application of SKF had no significant effect on current amplitude (4.5 ± 3.2% decrease) in these cells ($n = 6$; $p > 0.05$; **Figure 9B**). Similarly to cells expressing Kv1.2 and Sig-1R and cells expressing Kv1.2 and eYFP, treatment with SKF had no significant effect on Kv1.2 inactivation in the presence of KvB2 ($n = 6$; $p > 0.05$; **Figure 9C**). These results are a strong indication that the effect of SKF on Kv1.2 channels is not due to direct block of the channel by SKF, but rather due to agonist-induced changes in Sig-1R activity.

Cells expressing Kv1.2, eYFP, and Kvβ2 retained heterogenous activation gating, with "slow" and "fast" cells both represented; however, the majority of cells exhibited "fast" activation gating (**Figure 9G**). Only one sampled cell displayed "slow" gating, with an activation tau of 10.7 ms at +60 mV ($n = 1$). "Fast" cells displayed an average activation tau of 1.2 ± 0.22 ms ($n = 8$; **Figure 9F-G**).

Our data suggest that co-expression of Kvβ2 with Kv1.2 blocks the effects of Sig-1R ligand-activation on Kv1.2. We speculate that this is due to physical occlusion of the Sig-1R binding site on Kv1.2, thus Sig-1R is no longer able to bind to the channel for regulatory purposes. This is further supported by the observation that Kvβ2-expressing cells were found to be primarily occupying the "fast" activation gating mode.

3.3.2 Competitive expression of Sig-1R and Kvβ2 restores Kv1.2 response to SKF

Taken together, our findings indicate that availability of Sig-1R to Kv1.2 may dictate activation gating mode. Overexpression of Sig-1R increases the number of "slow" cells in

comparison with cells endogenously expressing Sig-1R. Further, expression of Kvβ2, which physically occludes Sig-1R interaction with Kv1.2, switches cells to the primarily "fast" gating mode. Despite these observations, these results do not conclusively show that Sig-1R interacts with the Kv1.2 closed state to regulate activation gating. We speculated that if Sig-1R and Kvβ2 were co-expressed, Sig-1R may competitively interact with a population of Kv1.2 channels and "slow" gating would be restored due to displacement of Kvβ2.

To test this, cells were transfected with equimolar amounts of Kv1.2, Sig-1R and Kvβ2 and were subject to previously described electrophysiology experiments. Cells with Sig-1R and Kvβ2 in competition exhibited an irreversible 15.3 ± 2.02 % decrease in current amplitude at + 80 mV upon application of SKF ($n = 6$; $p < 0.0001$; **Figure 9D**), which is intermediate to cells expressing Kv1.2 and Sig-1R (28.2% decrease) and cells expressing Kv1.2, eYFP and Kvβ2 (4.2% decrease).

As the effect of Sig-1R ligand-activation on Kv1.2 channels was partially restored, we predicted that "slow" activation gating would again be present in a proportion of the sampled cells. As expected, competitive expression of Sig-1R with Kvβ2 restored "slow" activation gating, with a mean activation tau of 11.24 ± 1.93 ms observed in "slow" cells ($n = 10$), and a mean activation tau of 1.31 ± 0.38 ms in "fast" cells ($n = 3$; **Figure 9F**). Similarly to cells overexpressing Sig-1R in the absence of Kvβ2, the majority of cells occupied the "slow" gating mode in the presence of Kvβ2 (**Figure 9G**).

When Sig-1R and Kvβ2 are co-expressed, we find that the response of Kv1.2 to SKF is re-established and "slow" activation gating is once again observed in a larger proportion of cells. These results confirm that Sig-1R directly modulates Kv1.2 and are a strong indication that Sig-1R is necessary for Kv1.2 "slow" gating. Sig-1R may directly interact with Kv1.2 as an extrinsic

gating regulator or may act as a scaffold for other unidentified regulatory proteins. Overall, we suggest that Sig-1R is an atypical Kv1.2 regulatory ancillary subunit. Sig-1R modulates Kv1.2 current amplitude via a direct interaction, aids in trafficking of Kv1.2 to the plasma membrane (Kourrich et al., 2013; Delint-Ramirez et al., 2018), and provides of site for pharmacological modulation of the Kv1.2 α-subunits.

3.4 Aim 4: Implications of Sig-1R modulation of Kv1.2 in ALS16

3.4.1 Sig-1R-E102Q has decreased interaction with Kv1.2 as compared to WT Sig-1R

In this work, we have shown that Sig-1R directly interacts with Kv1.2 as a regulatory ancillary subunit to regulate channel biophysical properties. As dysfunction and deletion of Kv1.2 has been associated with various pathologies, including epilepsy and motor neuron disease (MND; Brew et al., 2007; Helbig et al., 2016; Robbins and Tempel, 2012; Shibuya et al., 2011), we sought to determine if aberrant modulation of Kv1.2 is also present in pathologies associated with Sig-1R dysfunction. Specifically, we wanted to examine how modulation of Kv1.2 may be altered in cells expressing the mutant Sig-1R underlying ALS16: Sig-1R-E102Q (Al-Saif et al., 2011).

` The Sig-1R-E102Q mutation results in the substitution of glutamine for glutamic acid in the linker region between the Sig-1R β2 and β3 regions (Schmidt et al., 2016). Although this mutation manifests as the loss of a single hydrogen bond in the final protein product (**Figure 10**), Sig-1R-E102Q has been known to display drastically different subcellular dynamics than the WT Sig-1R. Previous work in our laboratory has suggested that Sig-1R-E102Q may behave as a constitutively active Sig-1R, displaying aberrant localization and mobility (Wong et al., 2016).

As it has been speculated that Sig-1R-E102Q is a toxically overactive Sig-1R, and our data demonstrates that prolonged ligand-activation of Sig-1R leads to decreased interaction with Kv1.2

(**Figure 4**), we predicted that Sig-1R-E102Q may fail to interact with Kv1.2 in apFRET imaging experiments. Whilst WT Sig-1R shows reticular patterning which is localized to the ER in confocal imaging studies (Wong et al., 2016), Sig-1R-E012Q is known display decreased reticular patterning, to aggregate in large cytosolic puncta, and to exhibit a small amount of diffuse distribution within the nucleus. In our experiments, photobleaching of mCh for apFRET was split into reticular Sig-1R-E102Q (**Figure 11A**) and Sig-1R-E102Q puncta (**Figure 11B**) as they have been shown to display differential mobility in FRAP experiments, with Sig-1R-E102Q puncta displaying decreased fluorescence recovery (Wong et al., 2016). We speculated that that dissimilar localization of Sig-1R-E102Q may indicate variability in the interaction with Kv1.2 channels.

In cells with reticular Sig-1R-E102Q expression, it was found that FRET efficiency was 8.1 ± 0.94%, which was a significant decrease in FRET efficiency as compared to WT Sig-1R expressing cells ($n = 29$; $p < 0.0001$; **Figure 11C**). Although Sig-1R-E102Q-mCh puncta consistently coincided with Kv1.2-GFP puncta, FRET efficiency was found to be 6.04 ± 0.81%, which was again a significant decrease in FRET efficiency as compared to WT Sig-1R ($n = 20$; $p < 0.0001$; **Figure 11C**). There was no difference in FRET efficiency between reticular and puncta Sig-1R-E102Q-mCh ($p = 0.31$), indicating that both groups similarly interact with Kv1.2-GFP.

Our apFRET data was further analyzed to examine FRAP of reticular and puncta Sig-1R-E102Q-mCh. We found that reticular Sig-1R-E102Q-mCh showed increased mobility as compared to WT Sig-1R, and Sig-1R-E102Q-mCh puncta showed similar mobility to WT Sig-1R (**Figure 11D**). We further show that application of SKF to cells expressing Sig-1R-E102Q-mCh and Kv1.2-GFP has no effect on apFRET or FRAP as compared to untreated cells (**Figure 12**). We previously associated increased Sig-1R mobility with prolonged agonist application

(**Figure 4**), thus these findings support the notion that Sig-1R-E102Q is a toxically overactive Sig-1R. Furthermore, our results corroborate Wong et al. (2016) and show that Sig-1R-E102Q puncta are largely immobile cytosolic aggregates.

3.4.2 Kv1.2 shows no electrophysiological response to SKF in cells expressing Sig-1R-E102Q

Our apFRET experiments show that Sig-1R-E102Q displays decreased interaction with Kv1.2, but they are not able to determine if this is coupled with aberrant modulation of Kv1.2 biophysical properties. Thus, our final line of experimentation was to obtain electrophysiological recordings from cells expressing Kv1.2 and Sig-1R-E102Q.

Cells expressing Kv1.2 and Sig-1R-E102Q-YFP were characterized in the presence and absence of SKF, as previously described. We observed a 5.1 ± 4.3% decrease in Kv1.2 current amplitude at + 80 mV upon treatment with SKF, which was deemed non-significant ($n = 5$; $p = 0.965$; **Figure 13A**). Similarly to all other sampled groups, treatment with SKF had no effect on Kv1.2 voltage-dependency of inactivation (n =5; **Figure 13B**).

As we previously determined that Sig-1R is necessary for Kv1.2 “slow” activation gating, we next looked at this property in cells expressing Sig-1R-E102Q. It was found that the majority of cells exhibited “fast” activation gating, with only two cells exhibiting “slow” activation gating (**Figure 13E**). Interestingly, the difference in voltage-dependency of activation and activation kinetics between “fast” and “slow” cells was less pronounced in Sig-1R-E102Q expressing cells than in all other groups examined (**Table 2**). “Fast” cells displayed a 1 mV leftward shift in $V_{1/2}$ of activation (**Figure 13C**) and displayed an average activation tau of 1.53 ± 0.18 ms at +60 mV ($n = 8$), and the “slow” cells within the population displayed a mean activation tau of 5.5 ms at +60 mV ($n = 2$).

These data demonstrate that when cells are expressing Sig-1R-E102Q, modulation of Kv1.2 by Sig-1R is disrupted. Ligand-activation of WT Sig-1R has been shown decrease Kv1.2 current amplitude, but this effect is abolished in Sig-1R-E102Q expressing cells. Further, our data demonstrates that overexpression of WT Sig-1R increases the proportion of cells displaying "slow" activation gating (Figure 5), but when Sig-1R-E102Q is overexpressed, cells are more likely to show "fast" activation gating. Overall, these results are an indication that Sig-1R-E102Q is not able to properly modulate Kv1.2 at baseline or upon ligand-activation.

4. DISCUSSION

This thesis attempted to define the interaction of Sig-1R with Kv1.2. Several studies have determined that ligand-activation of Sig-1R modulates the functionally and structurally similar Kv1.3. Kv1.4 and Kv1.5 channels, but this was the first work to explore Kv1.2 biophysical properties in response to Sig-1R activation. This study investigated the claim that Sig-1R is a "ligand-regulated Kv1.x auxiliary subunit" (Aydar et al., 2002) and found that expression of a Kvβ-subunit can occlude the regulatory interaction of Sig-1R with Kv1.2, suggesting a physical blockade of the Sig-1R binding site on Kv1.2 or a common locus of interaction. Further, this thesis aimed to investigate the relationship between the mutant Sig-1R underlying ALS16 and Kv1.2 channels, with the overarching goal of identifying a novel mechanism of disease pathophysiology.

How does ligand-activation of Sig-1R regulate Kv1.2?

Sig-1R regulation of Kv1 channels has shown to be dynamic and subtype dependent: acute application of Sig-1R agonists may decrease potassium conductance through Kv1 channels, accelerate Kv1 channel inactivation (Aydar et al., 2002), or have no discernable effect (Kinoshita et al., 2012). The mere expression of Sig-1R has further been shown to regulate Kv1 channels (Kinoshita et al., 2012), indicating a role for Sig-1R modulation of Kv1 channels at baseline. Moreover, due to the ability of Sig-1R to promiscuously bind to a variety of ligands, the action of the ligand-activated Sig-1R may be dependent on the specific ligand. For instance, Kourrich et al. (2012) show that chronic treatment with cocaine promotes the interaction between Sig-1R and Kv1.2, but we show that prolonged treatment with SKF decreases the interaction between Sig-1R and Kv1.2. Although several mechanisms of regulation have been identified in recombinant systems, Sig-1R modulation of Kv1 channels is still largely uncharacterized. Here, we find that

Sig-1R interacts with Kv1.2 at baseline and upon ligand activation. Additionally, we show that acute Sig-R ligand application decreases Kv1.2 current amplitude in voltage-clamp recordings.

This study represents the first biophysical characterization of Kv1.2 in response to Sig-1R ligand-activation. Further, we show novel data that the effect of Sig-1R ligand-activation may be occluded in the presence of the Kvβ2 regulatory subunit. It was previously suggested that Sig-1R is a ligand-regulated Kv1 auxiliary subunit, and here we present novel findings that expression of the Kv1 specific subunit Kvβ2 blocks the regulatory effects of Sig-1R on Kv1.2. These findings suggest that Sig-1R physically associates with Kv1.2 for modulatory purposes, and that Sig-1R behaves as an atypical Kv1.2 auxiliary subunit.

Although this study was performed in HEK293 cells recombinantly expressing Kv1.2, it has been previously shown that that the interaction between Sig-1R and Kv1.2 is a conserved cellular mechanism which extends to non-neuronal systems (Delint-Ramirez et al., 2018); thus, we can confidently speculate that our identified regulatory mechanisms will extend to neuronal cells. As Kv1 channels often co-assemble as heterotetramers, the identified regulatory mechanisms of Kv1.2 will apply to the other Kv1 channels in an endogenous expression system. Heterogenous assembly in the Kv1 family adds additional layers of control and plasticity, and combinations of Kv1 subtypes may harness unique regulatory pathways (Po et al., 1993; Nitabach et al., 2000; Baronas et al., 2015).

Although Sig-1R is known to be subject to activation by ligands, it may also be activated in other contexts, such as ER stress. Future work may determine if ligand-independent mechanisms of Sig-1R activation induce modulation of Kv1 channels. These results would contribute to the known role of Sig-1R as an interorganelle signalling molecule and would provide insight to Sig-1R behaviour in a dynamic cellular environment.

Is Sig-1R involved in Kv1.2 bimodal activation gating?

It has been suggested that the presence of Kv1.2 in Kv1 heteromers is particularly important within the Kv1 family for determining the membrane voltage required for channel activation (Brew et al., 2007, Baronas et al., 2015). As Kv1 channel activation is required for the descending phase of an action potential, the mechanisms of control of Kv1.2 activation gating play a distinct and vital role in maintaining appropriate neuronal excitability. The ability of Kv1.2 to switch gating mode in response to repetitive trains of action potentials (Baronas et al., 2015) is a mechanism of acute plasticity which contributes to the adaptability of Kv1.2 expressing neurons.

Changes in regulation and expression of Kv1.2 are associated with diseases of excitability. In a seizure-prone gerbil model, Kv1.2 is downregulated, whilst other delayed-rectifier channels are unaffected (Lee et al., 2009). It has also been noted that reduced delayed-rectifier potassium channel current is found in hyperexcitable motor neurons (Waigner et al., 2014), which is further correlated with the specific decrease in Kv1.2 staining (Shibuya et al., 2011). At the neuronal level, the presence of Kv1.2 has a strong dampening force in the regulation of action potential firing in the hippocampus (Palani et al., 2010). To this end, we predict that decreased expression of Kv1.2 has the same neuronal effect as dysfunctional regulation of Kv1.2 activation gating. Barons et al. (2015) suggest that the physiological consequence of Kv1.2 bimodal activation is to suppress excitability in a use-dependent manner. Disruptions of Kv1 channel homeostasis by the altered function of Kv1.2 heterogenous activation gating may be a hitherto uncharacterized mechanism of hyperexcitability: because activation gating plasticity is absent, cells have an artificially high threshold for firing and an impaired ability to adapt to repetitive stimuli.

The variability in Kv1.2 channel activation gating mode is attributed to a regulatory process rather than an intrinsic property of the channel (Baronas et al., 2016). Here, we show that

availability of Sig-1R to Kv1.2 is correlated with the prominent activation-gating mode in recombinant cells, and we further confirm that Sig-1R and Kv1.2 interact directly. Although our results do not show that Sig-1R is the lone regulator of Kv1.2 bimodal activation gating, they are a strong indication that Sig-1R is required for Kv1.2 to occupy the "slow" gating mode. The biophysical consequences of Sig-1R association with Kv1.2 enhances our understanding of Sig-1R control of action potential propagation and of Kv1.2 in limiting repetitive firing and protecting against hyperexcitability. These findings are particularly novel and will be an interesting future point of study to determine a precise mechanism of regulation.

Why do Sig-1R mutations have increased disease burden in motor neurons?

Excitotoxicity in MND describes neuronal hyperexcitability leading to a toxic increase of intracellular calcium (Pasinelli and Brown, 2006). It has been shown that the observed increase of free calcium within motor neurons is upstream of ER-stress pathways, which may trigger the Unfolded Protein Response (UPR) leading to cell death cascades (Kiskinis et al., 2014). Although "excitotoxicity" refers to increased glutamate in excitatory synapses, hyperexcitability in axons has also been found in MND patients (Nakata et al., 2006), and the degree of hyperexcitability in axons is further known to correlate with patient survival (Kanai et al., 2012). It has been proposed that axonal hyperexcitability is due to a mechanism involving decreased activity of delayed-rectifier potassium channels (Kanai et al., 2006).

Many lines of evidence point to specific role for Kv1.2 in the protection against hyperexcitability in MND. As previously mentioned, a recurrent LOF mutation in KCNA2 results in hereditary spastic paraplegia (HSP; Helbig et al., 2016). Moreover, it has been observed that delayed-rectifier potassium channel current is reduced in ALS-patient motor neurons derived from

iPSCs (Wainger et al., 2014), and there are reduced levels of Kv1.2 in patients with sporadic ALS, as determined by post-mortem IHC (Shibuya et al., 2011). We speculate that Kv1.2 – with its unique ability to display bimodal activation gating – may be disproportionately important among the Kv1 family in protecting against motor neuron hyperexcitability via use-dependent suppression of excitability (Baronas et al., 2015). Thus, the investigation of the role of Kv1.2 in MND may provide valuable insights to disease pathogenesis.

In this study, we aimed to determine how expression of the ALS16-causing Sig-1R-E102Q mutant may alter the effect of Sig-1R ligand-activation on Kv1.2 biophysical properties. We find that application of SKF does not facilitate a Sig-1R dependent decrease in Kv1.2 current amplitude. We further show that recombinant cells expressing Sig-1R-E102Q and Kv1.2 exist primarily in the "fast" activation gating mode. Paired with the finding that Sig-1R-E102Q displays decreased interaction with Kv1.2, these results are an indication that the E102 residue is required for Sig-1R modulation of Kv1.2 and for Kv1.2 to occupy the "slow" gating mode. We predict that the loss of this modulatory interaction disables the ability of Kv1.2 to display acute plasticity and interferes with the adaptability of Kv1.2 to repetitive trains of action potentials. Although it is difficult to make physiological predictions from recombinant models, our data may indicate that there is a failure of Kv1.2 to suppress excitability in the axons of motor neurons afflicted with the SIGMAR1 mutation underlying ALS16.

Gene mutations in SIGMAR1 exclusively result in MND (Al-Saif et al., .2011; Li et al., 2015) but Sig-1R is ubiquitously expressed throughout the human body. Sig-1R-E102Q is the most characterized of the SIGMAR1 mutations underlying MND (Fukunaga et al., 2015; Wong et al., 2016; Dresser et al., 2017); however, the selective death of motor neurons is not understood and has not been investigated. It has been proposed that Sig-1R-E102Q mediated ALS16 pathogenesis

is due to altered ER function and subsequent impaired protein homeostasis (Dresser et al., 2017), but this account is not entirely pleasing as ER-stress pathways are common to all cell types. Thus, we propose that dysfunctional cellular excitability is upstream of ER-stress mediated pathways. As Sig-1R is expressed in almost all tissue and cell types, and Sig-1R mutations exclusively exhibit MND phenotypes, we aimed to investigate a mechanism of pathophysiology which may underlie the specific death of motor neurons and may explain why protein homeostasis is disproportionately affected in these cells. Given that reduced delayed-rectifier potassium channel current is a mechanism of hyperexcitability in ALS patient-derived motor neurons (Waigner et al., 2014), and that hyperexcitability triggers an increase of intracellular calcium leading to ER-stress associated cell death cascades (Pasinelli and Brown, 2006; Kiskinis et al., 2014), we predict that dysfunctional cellular excitability via dysregulation of Kv1.2 by Sig-1R-E102Q may represent a hitherto uncharacterized mechanism of toxic hyperexcitability in ALS16.

5. CONCLUSION

This thesis further defined the role of Sig-1R as regulator of intrinsic neuronal excitability via modulation of Kv1.2 channels. I determined that Sig-1R directly interacts with Kv1.2 to modulate channel biophysical properties, in the presence and absence of ligand. This thesis begins to characterize the role of Sig-1R as a Kv1.2 regulatory ancillary subunit, which interacts with the pore-forming Kv1.2 α-subunits to modulate channel biophysical properties and creates a site for pharmacological manipulation of channel functionality. Further, my work beings to identify a novel mechanism of hyperexcitability in motor neurons of ALS16 patients, which is attributed to an aberrant interaction between Sig-1R-E102Q and Kv1.2. As Sig-1R interacts with Kv1.2 to regulate Kv1.2 heterogenous activation gating, I show preliminary evidence that this mechanism is disrupted in cells expressing the ALS16-causing Sig-1R-E102Q mutant.

This thesis represents a basic biophysical study which may guide future studies investigating the pathophysiology of Sig-1R-E102Q in increasingly complex systems. Although Kv1.2 and Sig-1R have vastly different roles in neuronal function, their dysfunction converges on MND phenotypes, and we speculate that this may be due to the role of Sig-1R as a Kv1.2 atypical axillary subunit, which modulates channel bimodal activation gating.

REFERENCES

Accili, E.A., J. Kiehn, Q. Yang, Z. Wang, A.M. Brown, and B.A. Wible. 1997. Separable Kvβ subunit domains alter expression and gating of potassium channels. *J Biol Chem*. 272(41): 25824—25831.

Accili, E.A., Y.A. Kuryshev, B.A. Wible, and A.M. Brown. 2004. Separable effects of human Kvβ1.2 N- and C-termini on inactivation and expression of human Kv1.4. *J Physiol*. 512(2): 325—336.

Al-Saif, A., F. Al-Mohanna, and S. Bohlega. 2011. A mutation in sigma-1 receptor causes juvenile amyotrophic lateral sclerosis. *Ann Neurol.* 70: 913—919.

Aydar, E., C.P. Palmer, V.A. Klyachko, and M.B. Jackson. 2002. The sigma receptor as a ligand-regulated auxiliary potassium channel subunit. *Neuron*. 34: 399—410.

Bajar, B.T., E.S. Wang, S. Zhang, M.L. Lin, and J. Chu. 2016. A guide to fluorescent protein FRET pairs. *Sensors.* 16: 1488.

Baronas, V.A., B.R. McGuinness, G.S. Brigidi, R.N. Gomm Kolisko, Y.Y. Vilin, R.Y. Kim, F.C. Lynn, S.X. Bamji, R. Yang, and H.T. Kurata. 2015. Use-dependent activation of neuronal Kv1.2 channel complexes. *J Neurosci.* 35(8): 3515—3524.

Baronas, V.A., R. Yang, Y.Y. Vilin, and H.T. Kurata. 2016. Determinants of frequency-dependent regulation of Kv1.2-containing potassium channels. *Channels*. 10(2): 158–166.

Bergeron, R., G. Debonnel, and C. De Montigny. 1993. Modification of N-methyl-D-aspartate response by antidepressant sigma receptor ligands. *Eur J Pharmacol*. 240(2-3): 319—323.

Brew, H.M., J.X. Gittelman, R.S. Silverstein, T.D. Hanks, V.P. Demas, L.C. Robinson, C.A. Robbins, J. McKee-Johnson, S.Y. Chiu, A. Messing, and B.L. Tempel. 2007. Seizures and reduced life span in mice lacking the potassium channel subunit Kv1.2, but hypoexcitability and enlarged Kv1 currents in auditory neurons. *J Neurophysiol.* 98: 1501—1525.

Browne, D. L, S.T. Grancher, J.G. Nutt, E.R. Brun, E.A. Smith, P. Kramer, and M. Litt. 1994. Episodic ataxia/myokymia syndrome is associated with point mutations in the human potassium channel gene, KCNA1. *Nat Gen.* 8(2): pp. 136-140.

Brownstein, M.J. 1993. A brief history of opiates, opioid peptides, and opioid receptors. *Proc Natl Acad Sci USA.* 90: 5391—5393.

Chen, X., Q. Wang, F. Ni, and J. Ma. 2010. Structure of the full-length Shaker potassium channel Kv1.2 by normal-mode-based X-ray crystallographic refinement. *Proc Natl Acad Sci USA.* 107(25): 11352—11357.

Choe, S. 2002. Potassium channel structures. *Nat Rev*. 3: 115—121.

Connor, J.X., K. McCormack, A. Pletsch, S. Gaeta, B. Ganetzky, S.Y. Chiu, and A. Messing. 2005. Genetic modifiers of the Kvβ2-null phenotype in mice. *Genes Brain and Beh.* 4: 77—88.

Crottes, D., S. Martial, R. Rapetti-Mauss, D.F. Pisani, C. Loriol, B. Pellissier, P. Martin, E. Chevet, F. Borgese, and O. Soriani. 2011. Sig1R protein regulates hERG channel expression through a post-translation mechanism in leukemic cells. *J Biol Chem.* 286: 27947—27958.

Cushman, S.J., M.H. Nanao, A.W. Jahng, D. DeRubeis, S. Choe, and P.J. Pfaffinger. 2000. Voltage dependent activation of potassium channels is coupled to T1 domain structure. *Nat Struct Biol*. 7: 403—407.

Delemotte, L., M. Tarek, M.L. Klein, C. Amaral, and W. Treptow. 2011. Intermediate states of the Kv1.2 voltage sensor from atomic molecular dynamics simulations. *Proc Natl Acad Sci USA.* 108: 6109—6114.

Delint-Ramirez, I., F. Garcia-Oscos, A. Segev, and S. Kourrich. 2018. Cocaine engages a non-canonical mechanism that controls neuronal excitability in the nucleus accumbens. *Mol Psych*. 10.1038.

Dodson, P.D., B. Billups, Z. Rusznak, G. Szucs, M.C. Barker, and I.D. Forsythe. 2003. Presynaptic rat Kv1.2 channels suppress synaptic terminal hyperexcitability following action potential invasion. *J Physiol.* 550(1): 27—33.

Doyle, D., A. Lee, J. Lewis, E. Kim, M. Sheng, and R. MacKinnon. 1996. Crystal structures of a complexed and peptide-free membrane protein binding domain: molecular basis of peptide recognition by PDZ. *Cell*. 85: 1067—1076.

Dresser, A., J.T. Vollrath, A. Sechi, S. Johann, A. Roos, A. Yamoah, I. Katona, S. Bohlega, D. Wiemuth, Y. Tian, A. Schmit, J. Vervoorts, M. Dohmen, C. Beyer, J. Anink, E. Aronica, D. Troost, J. Weis, and A. Goswami. 2017. The ALS-linked E102Q mutation in Sigma receptor-1 leads to ER stress-mediated defects in protein homeostasis and dysregulation of RNA-binding proteins. *Cell Death Differentiation*. 24: 1655—1671.

Fukunaga, K., Y. Shinoda, and H. Tagashira. 2015. The role of SIGMAR1 gene mutation and mitochondrial dysfunction in amyotrophic lateral sclerosis. *J Pharmacol Sci.* 127: 36—41.

Gao, X.F., J.J. Yao, Y.L. He, C. Hu, and Y.A. Mei. 2012. Sigma-1 receptor agonists directly inhibit Nav1.2/1.4 channels. *PLoS One.* 7: e49384.

Grissmer, S., A.N. Nguyen, J. Aiyar, D.C. Hanson, R.J. Mather, G.A. Gutman, M.J. Karmilowicz, D.D. Auperin, and K.G. Chandy. 1994. Pharmacological characterization of five cloned voltage-gated K+ channels, types Kv1.1, 1.2, 1.3, 1.5, and 3.1, stably expressed in mammalian cell lines. *Mol Pharmacol*. 45: 1227—1234.

Hanner, M., F.F. Moebius, A. Flandorfer, H.G. Knaus, J. Striessnig, E. Kempner, and H. Glossmann. 1996. Purification, molecular cloning, and expression of the mammalian σ1-binding site. *Proc Natl Acad Sci USA.* 93: 8072—8077.

Hayashi, T., and T.P. Su. 2003. Intracellular dynamics of sigma-1 receptors (σ1 binding sites) in NG108-15 cells. *J Pharmacol Exp Ther.* 306: 726—733.

Hayashi, T. and T.P. Su. 2004. Sigma-1 receptors at galactosylceramide-enriched lipid microdomains regulate oligodendrocyte differentiation. *Proc Natl Acad Sci USA.* 101: 14949—14954.

Hayashi, T., and T.P. Su. 2007. Sigma-1 receptor chaperones at the ER mitochondrion interface regulated Ca2+ signaling and cell survival. *Cell*. 131: 596—610.

Heinemann, S.H., J. Rettig, H.R. Graack, and O. Pongs. 1996. Functional characterization of Kv channel β-subunits from rat brain. *J Physiol*. 493(3): 625—633.

Helbig, K.L., U.B.S. Hedrich, D.N. Shinde, I. Krey, A.C. Teichmann, J. Hentschel, J. Schubert, A.C. Chamberlin, R. Huether, H.M. Lu, W.A. Alcaraz, S. Tang, C. Jungbluth, S.L. Dugan, L. Vainionpaa, K.N. Karle, M. Synofzik, L. Schols, R. Schule, A.E. Lehesjoki, I. Helbig, H. Lerche, and J.R. Lemke. 2016. A recurrent mutation in KCNA2 as a novel cause of hereditary spastic paraplegia and ataxia. *Ann Neurol*. 80(4): 638—642.

Hodgkin, A.L., and A.F. Huxley. 1952a. A quantitative description of membrane current and its application to conduction and excitation in nerve. *J Physiol.* 117(4): 500—544.

Hodgkin, A.L., and A.F. Huxley. 1952b. Currents carried by sodium and potassium ions through the membrane of the giant axon. *J Physiol.* 116(4): 449—472.

Horne, A.J., C.J. Peters, T.W. Claydon, and D. Fedida. 2010. Fast and slow voltage sensor rearrangements during activation gating in Kv1.2 channels detected using tetramethylrhodamine fluorescence. *J Gen Physiol.* 136(1): 83–99.

Ishida. I.G., G.E. Rangel-Yescas, J. Carrasco-Zanini, and L.D. Islas. 2015. Voltage-dependent gating and gating charge measurements in the Kv1.2 potassium channel. *J Gen Physiol*. 145(4): 345–358.

Jan, L.Y, and Y.N. Jan. 2012. Voltage-gated potassium channels and the diversity of electrical signalling. *J Phyiol.* 590(11): 2591—2599.

Jansen, K.L.R., R.L.M. Faull, M. Dragunow, and R.A. Leslie. 1991. Autoradiographic distribution of sigma receptors in human neocortex, hippocampus, basal ganglia, cerebellum, pineal and pituitary glands. *Brain Res*. 559: 172—177.

Kanai, K., S. Kuwabara, S. Misawa, N. Tamura, K. Ogawara, M. Nakata, S. Sawai, T. Hattori, and H. Bostock. 2006. Altered axonal excitability properties in amyotrophic lateral sclerosis: impaired potassium channel functional related to disease stage. *Brain*. 129: 953—962.

Kanai, K., K. Shibuya, Y. Sato, S. Misawa, S. Nasu, Y. Sekiguchi, S. Mitsuma, S. Isose, Y. Fujimaki, and S. Ohmori. 2012. Motor axonal excitability properties are strong predictors for survival in amyotrophic lateral sclerosis. *J Neurol Neurosurg Psychiatry.* 83: 734—738.

Kim, D.M., and C.M. Nimigean. 2016. Voltage-gated potassium channels: a structural examination of selectivity and gating. *Cold Spring Harb Perspect Biol*. 8: 1—19.

Kinoshita, M., Y. Matsuoka, T. Suzuki, J. Mirrielees, and J. Yang. 2012. Sigma-1 receptor alters the kinetics of Kv1.3 voltage gated potassium channels but not the sensitivity to receptor ligands. *Brain Res.* 1452: 1—9.

Kiskinis, E., J. Sandoe, L.A. Williams, G.L. Boulting, R. Moccia, B.J. Wainger, S. Han, T. Peng, S. Thams, S. Mikkilineni, C Mellin, F.T. Merkle, B.N. Davis-Dunsenbery, M. Ziller, D. Oakley, J. Ichida, S. Di Costanzo, N. Atwater, M.L. Maeder, M.J. Goodwin, J. Nemesh, R.E. Handsaker, D. Paull, S. Noggle, S.A. McCarroll, J.K. Joung, C.J. Woolf, R.H. Brown, and K. Eggan. 2014. Pathways disrupted in human ALS motor neurons identified through genetic correction of mutant SOD1. *Cell Stem Cell* 14: 781—795.

Kourrich, S., T. Hayashi, J.Y. Chuang, S.Y. Tsai, T.P. Su, and A. Bonci. 2013. Dynamic interaction between Sigma-1 receptor and Kv1.2 shapes neuronal and behavioural responses to cocaine. *Cell.* 152: 236—247.

Kourrich, S., 2017. Sigma-1 receptor and neuronal excitability. *Handbook of Experimental Pharmacology*. 224: 109—130.

Kuo, J.J., M. Schonewille, T. Siddique, A.N. Schults, R. Fu, P.R. Bar, R. Anelli, C.J. Heckman, and A.B. Kroese. 2004. Hyperexcitability of cultured spinal motorneurons from presymptomatic ALS mice. *J Neurophysiol*. 91: 571—575.

Lam, A.J., F. St-Pierre, Y. Gong, J.D. Marshall, P.J. Cranfill, M.A. Baird, M.R. McKeown, J. Wiedenmann, M.W. Davidson, M.J. Schnitzer, R.Y. Tsien, and M.Z. Lin. 2012. Improving FRET dynamic range with bright green and red fluorescent proteins. *Nat Methods*. 9: 1005—1012.

Lee, S.M., J.E. Kim, J.H. Sohn, H.C. Choi, J.S. Lee, S.H. Kim, M.J. Kim, I.G. Choi, and T.C. Kang. 2009. Down-regulation of delayed rectifier K+ channels in the hippocampus of seizure sensitive gerbils. *Brain Res Bul*. 40(6): 433—442.

Leung, Y.M. 2012. Involvement of C-type inactivation gating in the actions of voltage-gated K+ channel inhibitors. *Pharm and Ther*. 133: 151—158.

Li, X., Z. Hu, L. Liu, Y. Xie, Y. Zhan, X. Zi, J. Wang, L. Wu, K. Xia, B. Tang. … 2015. A SIGMAR1 splice-site mutation causes distal hereditary motor neuropathy. *Neurology*. 84: 2430—2437.

Liman, E.R., P. Hess, F. Weaver, and G. Koren. 1991. Voltage sensing residues in the S4 region of a mammalian Kv1 channel. *Nature*. 353: 752—756.

Long, S.B., E.B. Campbell, and R. Mackinnon. 2005a. Crystal structure of a mammalian voltage-dependent Shaker family K+ channel. *Science.* 309: 897—903.

Long, S.B., E.B. Campbell, and R. MacKinnon. 2005b. Voltage sensor of Kv1.2: structural basis of electromechanical coupling. *Science*. 309: 903—908.

Martin, K.J., E.J. McGhee, J.P. Schwarz, M. Drysdale, S.M. Brachmann, V. Stucke, O.J. Sansom, and K.I. Anderson. 2018. Accepting from the best donor; analysis of long-lifetime donor fluorescent protein pairings to optimise dynamic FLIM-based FRET experiments. *PLoS One.* 13(1): e0183538.

Matsumoto, R.R., W.D. Bowen, and T.P Su. 2007. Sigma receptors: chemistry, cell biology and clinical implications. *Springer.*

Mavlyutov, T.A., and Ruoho A.E. 2007. Ligand-dependent localization and intracellular stability of sigma-1 receptors in CHO-K1 cells. *J Mol Signal*. 2: 8.

Mavlyutov, T.A., L.W. Guo, M.L. Epstein, and A.E. Ruoho. 2015. Role of sigma-1 receptor in amyotrophic lateral sclerosis (ALS). *J Pharmacol Sci*. 127: 10—16.

Mavlyutov, T.A., X. Chen, L. Guo, and J. Yang. 2017. APEX2-tagging of sigma 1-receptor indicates subcellular protein topology with cytosolic N-terminus and ER luminal C-terminus. *Protein Cell*. doi: 10.1007/s13238-017-0468-5.

McCormack, T., K. McCormack, M.S. Nadal, E. Vieira, A. Ozaita, and B. Rudy. 1999. The effects of Shaker β-subunits on the human lymphocyte K+ channel Kv1.3. *J Biol Chem.* 274(29):20123—20126.

Nakahira, K., G. Shi, K.J. Rhodes, and J.S. Trimmer. Selective interaction of voltage-gated K+ channel β-subunits with α-subunits. *J Biol Chem.* 271(12): 7084—7089.

Nakata, M., S. Kuwabara, K. Kanai, S. Misawa, N. Tamura, S. Sawai, T. Hattori, and H. Bostock. 2006. Distal excitability changes in motor axons in amyotrophic lateral sclerosis. *Clin Neurophysiol.* 117: 1444—1448.

Nguyen, L., N. Kaushal, M.J. Robson, and R.R. Matsumoto. 2014. Sigma receptors as potential therapeutic targets for neuroprotection. *Eur J Pharmacol*. 743: 42—47.

Nitabach, M.N., D.A. Llamas, R.C. Araneda, J.L. Intile, I.J. Thompson, Y.I. Zhou, and T.C. Holmes. 2001. A mechanism for combinatorial regulation of electoral activity: potassium channel subunits capable of functioning as Src homology 3-dependent adaptors. *Proc Natl Acad Sci USA*. 98: 705—710.

Organ-Darling, L.E., A.N. Vernon, J.R. Giovanniello, Y. Lu, K. Moshal, K. Roder, W. Li, and G. Koren. 2013. Interactions between hERG and KCNQ1 α-subunits are mediated by their COOH termini and modulated by cAMP. *Am J Physiol Heart Circ Physiol.* 304: H589—H599.

Palani, D., A. Baginskas, and M. Raastad. 2010. Bursts and hyperexcitability in non-myelinated axons of the rat hippocampus. *Neurosci*. 167(4): 1004—1013.

Pasinelli, P., and R.H. Brown. 2006. Molecular biology of amyotrophic lateral sclerosis: insights from genetics. *Nat Rev Neurosci*. 7: 710—723.

Pena, S.D., and R.L. Coimbra. 2015. Ataxia and myoclonic epilepsy due to a heterozygous mutation in KCNA2: proposal for a new channelopathy. *Clin Genet*. 87: e1—e3.

Peri, R., B.A. Wible, and A.M. Brown. 2001. Mutations in the Kvβ2 binding site for NADPH and their effects on Kv1.4. *J Biol Chem*. 276(1): 738—741.

Po, S., S. Roberds, D.J. Snyders, M.M. Tamkun, and P.B. Bennett. 1993. Heteromultimeric assembly of human potassium channels. Molecular basis of a transient outward current? *Circ Res*. 72: 1326—1336.

Pongs, O., and J.R. Schwarz. 2010. Ancillary subunits associated with voltage-dependent K+ channels. *Physiol Rev*. 90: 755—796.

Rasband, M.N. 2010. Clustered Kv channel complexes in axons. *Neurosci Lett*. 486: 101—106.

Rettig, J., S.H. Heinemann, F. Wunder, C. Lorra, D.N. Parcej, O. Dolly, and O. Pongs. 1994. Inactivation properties of voltage-gated K+ channels altered by presence of β-subunit. *Nature*. 369: 289—294.

Rezazadeh, S., H.T. Kurata, T.W. Claydon, S.J. Kehl, and D. Fedida. 2007. An activation gating switch in Kv1.2 is localized to threonine residue in the S2-S3 linker. *Biophys J*. 93: 4173–4186.

Robbins, C.A., and B.L. Tempel. 2012. Kv1.1 and Kv1.2: similar channels, different seizure models. *Epilepsia*. 53(1): 134—141.

Schmidt, H.R., S. Zheng, E. Gurpinar, A. Koehl, A. Manglik, and A.C. Kruse. 2016. Crystal structure of the human σ1 receptor. *Nature*. 532: 527—530.

Schultz, D., M. Litt, L. Smith, M. Thayer, and K. McCormack. 1996. Localization of two potassium channel β subunit genes: KCNA1B and KCNA2B. *Genomics*. 31(3): 389-391.

Sewing, S., J. Roeper, and O. Pongs. 1996. Kvβ1 subunit binding specific for shaker-related potassium channel α subunits. *Neuron*. 16: 455—463.

Sharkey, J., K.A. Glen, S. Wolfe, and M.J. Kuhard. 1988. Cocaine binding at σ receptors. *Eur J Pharmacol*. 149(1-2): 171—174.

Shaw, P.J. 1994. Excitotoxicity and motor neurone disease: a review of the evidence. *J Neurolog Sci*. 124: 6—13.

Shibuya, K., S. Misawa, K. Arai, M. Nakata, K. Kunai, Y. Yoshiyama, K. Ito, S. Isose, Y. Noto, S. Nasu, Y. Sekiguchi, Y. Fujimaki, S. Ohmori, H. Kitamura, Y. Sato, and S. Kuwabara. 2011. Markedly reduced axonal potassium channel expression in human sporadic amyotrophic lateral sclerosis: an immunohistochemical study. *Exp Neurology*. 232: 149—153.

Smart, S.L., V. Lopantsev, C.L. Zhang, C.A. Robbins, H. Wang, S.Y. Chiu, P.A. Schwartzkroin, A. Messing, and B.L. Tempel. 1998. Deletion of the Kv1.1 potassium channel causes epilepsy in mice. *Neuron.* 20: 809—819.

Smith, S.B., J. Duplantier, Y. Dun, B. Mysona, P. Roon, P.M. Martin, and V. Ganapathy. 2008. In vivo protections against retinal neurodegeneration by sigma receptor 1 ligand +-pentazocine. *Invest Opthamol Vis Sci*. 49: 4154—4161.

Southan, A.P., and B. Robertson. 1998. Patch-clamp recordings from cerebellar basket cell bodies and the presynaptic terminals reveal an asymmetric distribution of voltage-gated potassium channels. *J Neurosci*. 18(3): 948—955.

Su, T.P., T. Hayashi, T. Maurice, S. Buch, and A.E. Ruoho. 2010. The sigma-1 receptor chaperone as an inter-organelle signalling modulator. *Trend Pharmacol Sci*. 31: 557—566.

Sutherland, M.L., S.H. Williams, R. Abedi, P.A. Overbeek, P.J. Pfaffinger, and J.L. Noebels. 1999. Overexpression of a Shaker-type potassium channel in mammalian central nervous system dysregulates native potassium channel gene expression. *Proc Natl Acad Sci USA.* 96: 2451—2455.

Syrbe, S., U.B.S. Hedrich, E. Riesch, T. Djemie, S. Muller, R.S. Moller, B. Maher, L. Hernandez-Hernandez, M. Synofzik, H.S. Caglayan, M. Arslan, J.M. Serratosa, M. Nothnagel, P. May, R. Krause, H. Loffler, K. Detert, T. Dorn, H. Vogt, G. Kramer, L. Schols, P.E. Mullis, T. Linnankivi, A.E. Lehesjoki, K. Sterbova, D.C. Craiu, D. Hoffman-Zacharska, C.M. Korff, Y.G. Weber, M. Steinlin, S. Gallati, A. Bertsche, M.K. Bernhard, A. Merkenschlager, W. Kiess, M. Gonzalez, S. Zuchner, A. Palotie, A. Suls, P. De Jonghe, I. Hebig, S. Biskup, M. Wolff, S. Maljevic, R. Schule, S.M. Sisodiya, S. Weckhuysen, H. Lerche, and J.R. Lemke. 2015. De novo loss- or gain-of-function mutations in KCNA2 cause epileptic encephalopathy. *Nat Genet*. 47: 393—399.

Tempel, B.L., Y.N. Jan, and L.Y. Jan. 1988. Cloning of a probably potassium channel gene from mouse brain. *Nature*. 332: 837—839.

VanDongen, A.M.J., G. Frech, J.A. Drewe, R.H. Joho, and A.M. Brown. 1990. Alteration and restoration of K1 channel function by deletions at the N- and C-termini. *Neuron*. 5: 433—443.

Wainger, B.J., E. Kiskinis, C. Mellin, O. Wiskow, S.S.W. Han, J. Sandoe, N.P. Perez, L.A. Williams, S. Lee, G. Boulting, J.D. Berry, R.H. Brown Jr., M.E. Cudkowicz, B.P. Bean,

K. Eggan, and C.J. Woolf. 2014. Intrinsic membrane hyperexcitability of ALS patient-derived motor neurons. *Cell Rep* 7(1): 1—11.

Wang, Z., J. Kiehn, Q. Yang, A.M. Brown, and B.A. Wible. 1996. Comparison of binding and block produced by alternatively spliced Kvβ1 subunits. *J Biol Chem.* 271: 28311—28317.

Watanabe, I., J. Zhu, J.J. Sutachan, A. Gottschalk, E. Recio-Pinto, and W.B. Thornhill. 2007. The glycosylation state of Kv1.2 potassium channels affect trafficking, gating, and simulated action potentials. *Brain Res.* 1144: 1—18.

Weissman, A.D., T.P. Su, J.C. Hedreen, and E.D. London. 1988. Sigma receptors in post-morten human brains. *J Pharmacol Exp Therapeutics*. 247(1): 29—33.

Wilke, R.A., P.J. Lupardus, D.K. Grandy, M. Rubinstein, M.J. Low, and M.B. Jackson. 1999. K+ channel modulation in rodent neurohypophysial nerve terminals by sigma receptors and not by dopamine receptors. *J Physiol*. 517.2: 291–406.

Wong, A.Y.C., E. Hristova, N. Ahlskog, L.A. Tasse, J.K. Ngsee, P. Chudalayandi, and R. Bergeron. 2016. Aberrant subcellular dynamics of sigma-1 receptor mutants underlying neuromuscular diseases. *Mol Pharmacol*. 90: 238—253.

Xu, J., and M. Li. 1997. Kvβ2 inhibits the Kvβ1-mediated inactivation of K+ channels in transfected mammalian cells. 1997. *J Biol Chem.* 272(18): 11728—11735.

Xu, J., P.A. Koni, P. Wang, G. Li, L. Kaczmarek, Y. Wu, Y. Li, R.A. Flavell, and G.V. Desir. 2003. The voltage-gated potassium channel K1.3 regulates energy homeostasis and body weight. *Hum Mol Genet*. 12(5): 551—559.

Yang, J.W., H. Vacher, K.S. Park, E. Clark, and J.S. Trimmer. 2007. Trafficking-dependent phosphorylation of Kv1.2 regulates voltage-gated potassium channel surface expression. *Proc Natl Acad Sci USA.* 104(50): 20055—20060.

Yellen, G. 2002. The voltage-gated potassium channels and their relatives. *Nature*. 419: 35—42.

Yoon, S.Y., D.H. Roh, H.S. Seo, S.Y. Kang, J.Y. Moon, S. Song, A.J. Beitz, and J.H. Lee. 2010. An increase in spinal dehydroepiandrosterone sulfate (DHEAS) enhances NMDA-induced pain via phosphorylation of the NR1 subunit in mice: involvement of the sigma-1 receptor. *Neuropharmacol*. 59(6): 460—467.

Zhang, H., and J. Cuevas. 2005. σ receptor activation blocks potassium channels and depressed neuroexcitability in rat intercardiac neurons. *J Pharmacol Exp Ther.* 313; 1387—1396.

Zadek, B., and C.M. Nimigean. 2006. Calcium-dependent gating of MthK, a prokaryotic potassium channel. *J Gen Physiol*. 127(6): 673—685.

Zhu, J., E. Recio-Pinto, T. Hartwig, W. Sellers, J. Yan, and W.B. Thornhill. 2009. The Kv1.2 potassium channel: the position of an N-glycan on the extracellular linkers affects its protein expression and function. *Brain Res.* 1251: 16—29.

Zukin, S.R., A. Tempel, E.I. Gardner, and R.S. Zukin. 1986. Interaction of [3H](—)-SKF-10.047 with brain sigma receptors: characterization and autoradiographic visualization. *J Neurochem.* 46: 1032—1041.

FIGURES

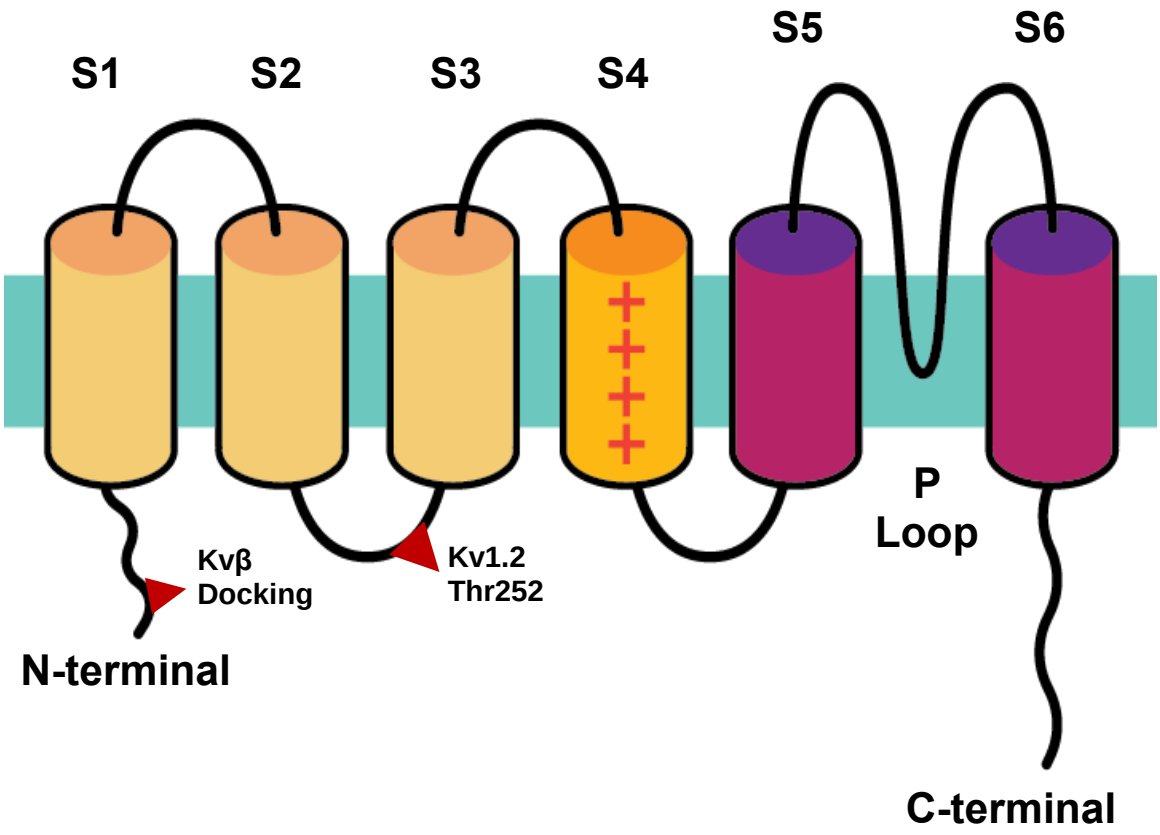

Figure 1. Schematic of a Kv1 (*Shaker*-type) voltage-gated potassium channel α-subunit. When expressed within the plasma membrane, each subunit of a Kv1 tetramer will have six transmembrane domains, denoted S1 trough S6. S1 – S4 contain the voltage-sensing region of the channel, whist S5 – S6 will compose the conduction region of the tetramer when functionally assembled. *Provided by M.E. Abraham, 2018.*

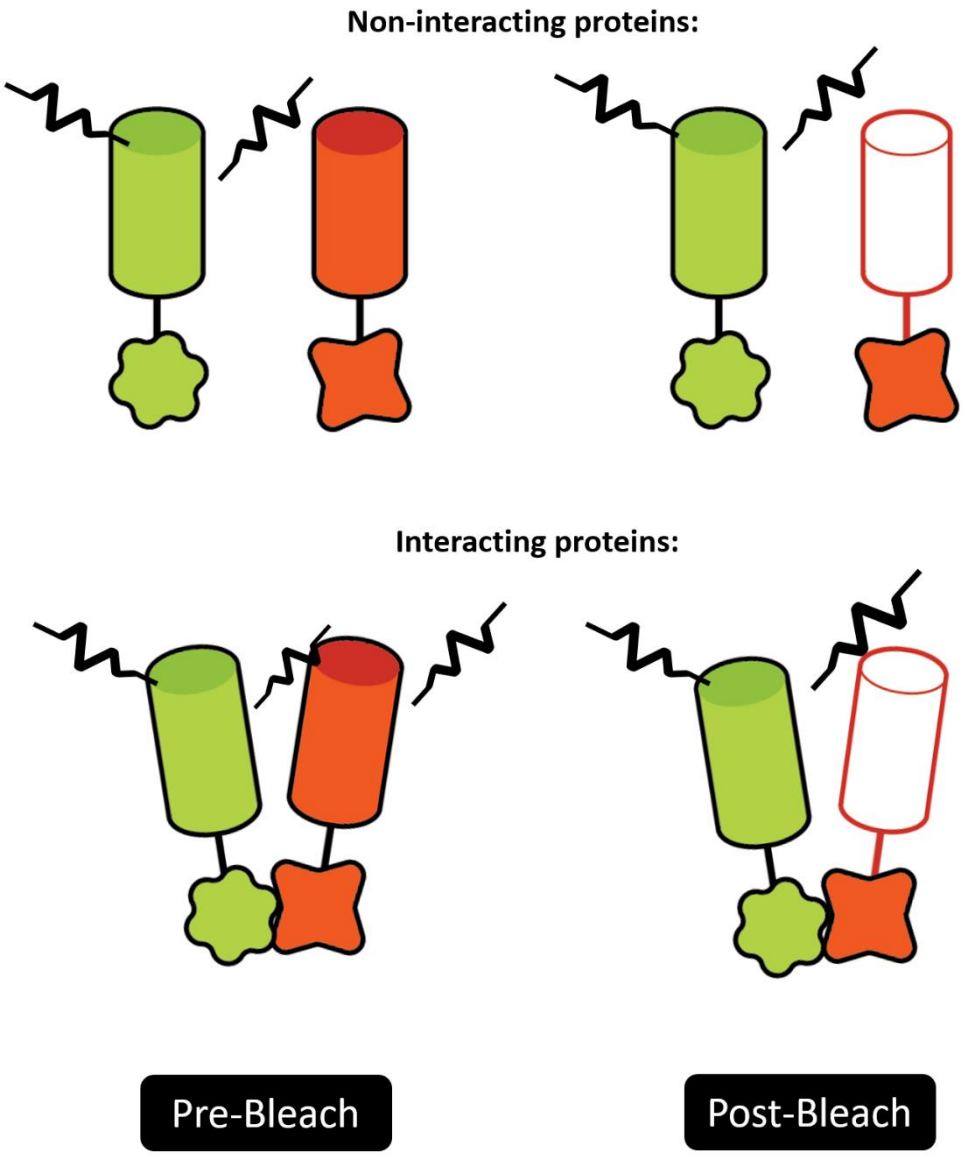

Figure 2: Schematic of acceptor-photobleaching FRET (apFRET). apFRET is dependent on emission energy transfer from the co-expressed fluorescent donor to the acceptor, such that excitation of the acceptor will quench donor emission when the proteins are in close proximity. With our chosen flourophores, Kv1.2-GFP is the fluorescent donor, and Sigma-mCh is the fluorescent acceptor. In a situation where the two proteins are not in close proximity, bleaching of mCh will have no effect on detected GFP emission. But if the proteins are sufficiently close (interacting), bleaching of mCh will cause an increase in detected GFP emission intensity. To this end, FRET efficiency can be calculated by measuring GFP emission intensity pre- and post- acceptor photobleaching. *Provided by M.E. Abraham, 2018.*

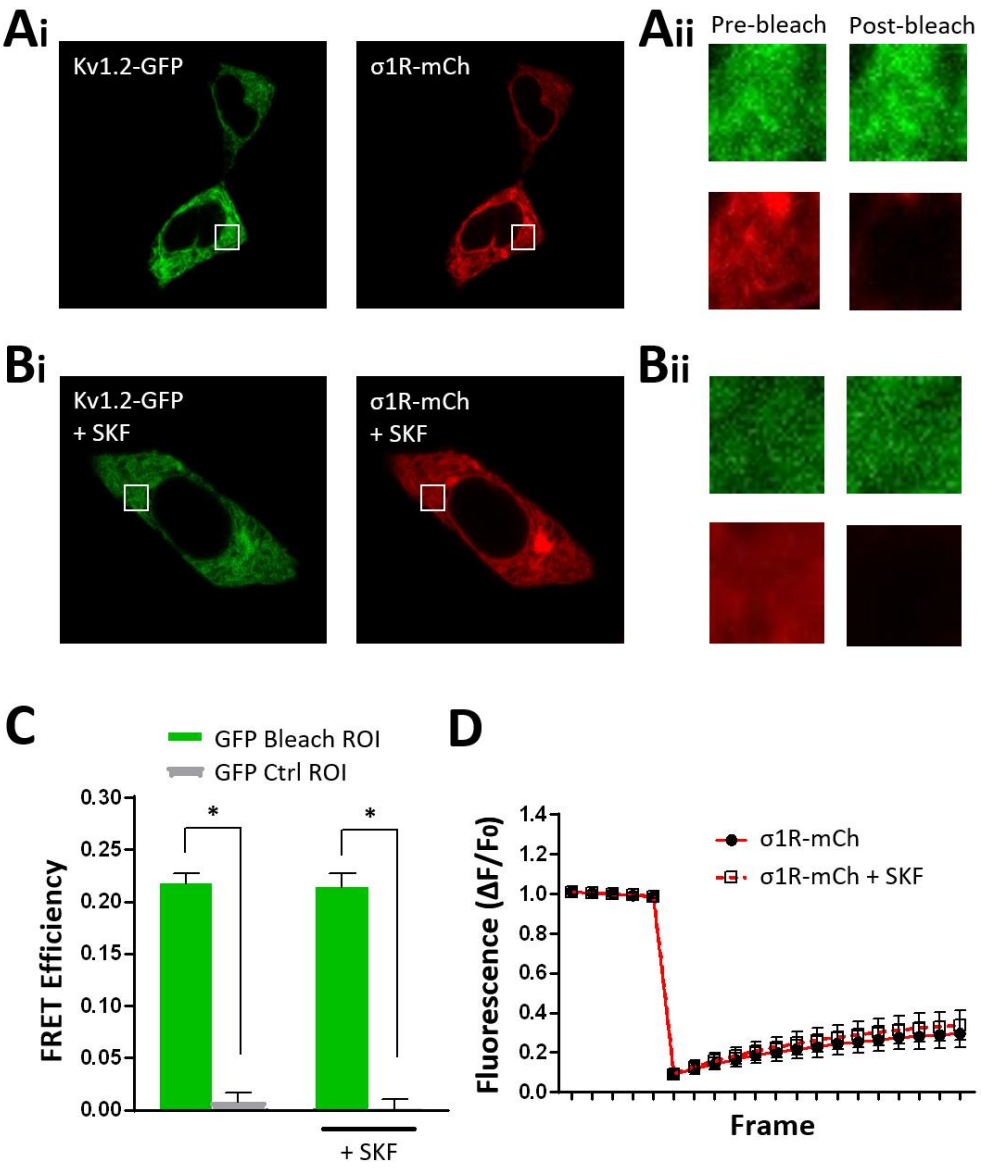

Figure 3: Kv1.2 and Sig-1R interact at baseline, and interaction is not further facilitated by acute Sig-1R ligand application. Representative confocal images of HEK293 cells transiently co-expressing Kv1.2-GFP and Sig-1R-mCh (**Ai**). Magnification of the square ROI displays Kv1.2-GFP and Sig-1R-mCh before and after acceptor photobleaching (**Aii**). HEK293 cells were additionally imaged in the presence of the Sig-1R agonist SKF (**B).** Quantification of the images shows a significant increase of FRET efficiency in the bleached ROI versus the control non-bleached ROI, and no significant differences between untreated and treated cells (**C**). Treated cells and untreated cells showed similar Fluorescence Recovery After Photobleaching of Sig-1R-mCh (**D**). Asterisks indicate statistical significance ($p < 0.05$).

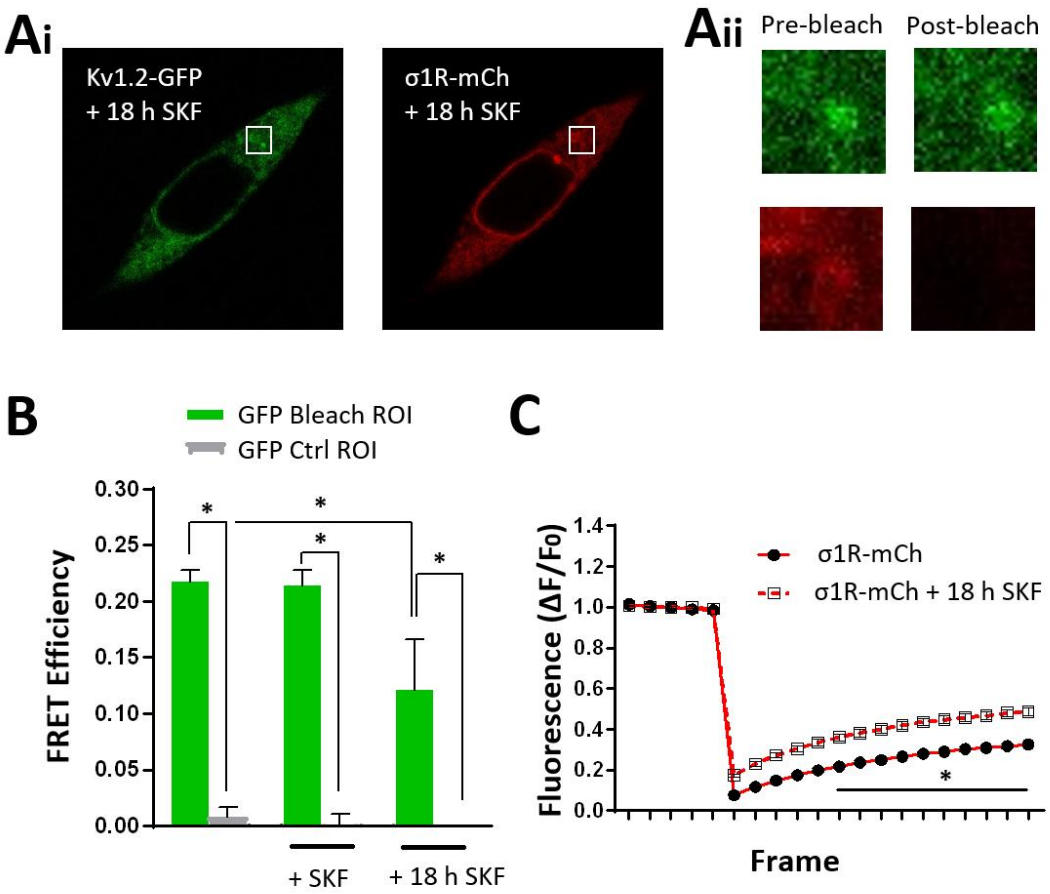

Figure 4: Kv1.2 and Sig-1R show decreased interaction following 18 h Sig-1R ligand treatment. Representative confocal images of HEK293 cells transiently co-expressing Kv1.2-GFP and Sig-1R-mCh, following 18 h SKF treatment, before and after acceptor photobleaching (**A**). When FRET efficiency was compared between the bleached regions in cells with no SKF treatment and 18 h SKF treatment, a significant decrease in FRET efficiency in 18 h SKF treated cells was found (**B**). Further, 18 h treated cells exhibited accelerated FRAP of Sig-1R-mCh as compared to untreated cells (**C**), indicating that prolonged SKF treatment increases Sig-1R mobility. Asterisks indicate statistical significance ($p < 0.05$).

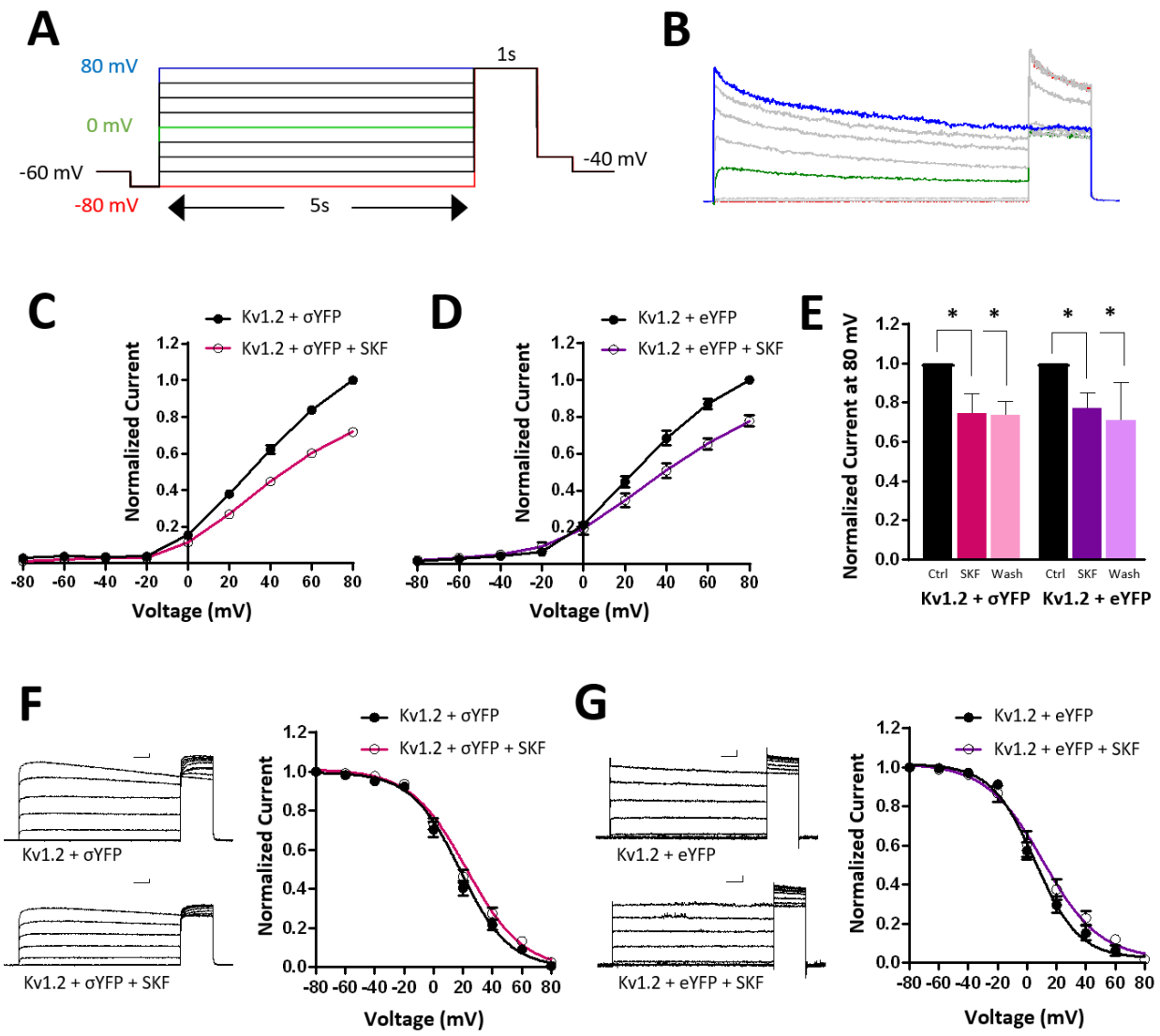

Figure 5: Effect of Sig-1R ligand-activation on cells overexpressing and endogenously expressing Sig-1R. Step protocol for determining Kv1.2 current-voltage relationship and voltage-dependency of inactivation (**A**). Raw traces were leak subtracted prior to analysis (**B**). Current voltage (IV) plots of cells expressing Kv1.2 and Sig-1R-YFP (**C**) or Kv1.2 and eYFP (**D**) show a significant decrease in current amplitude upon treatment with SKF (**C**), which was not reversed upon drug washout (**E**). Voltage-dependency of inactivation was calculated from leak subtracted traces for cells expressing Kv1.2 and Sig-1R-YFP (**F**), and cells expressing Kv1.2 and eYFP (**G**). Treatment with SKF caused no change in $V_{1/2}$ of inactivation in both cells expressing Kv1.2 and Sig-1R-YFP and cells expressing Kv1.2 and eYFP. Scalebar in all cases is 500 ms, 300 pA. Asterisks indicate statistical significance ($p < 0.05$).

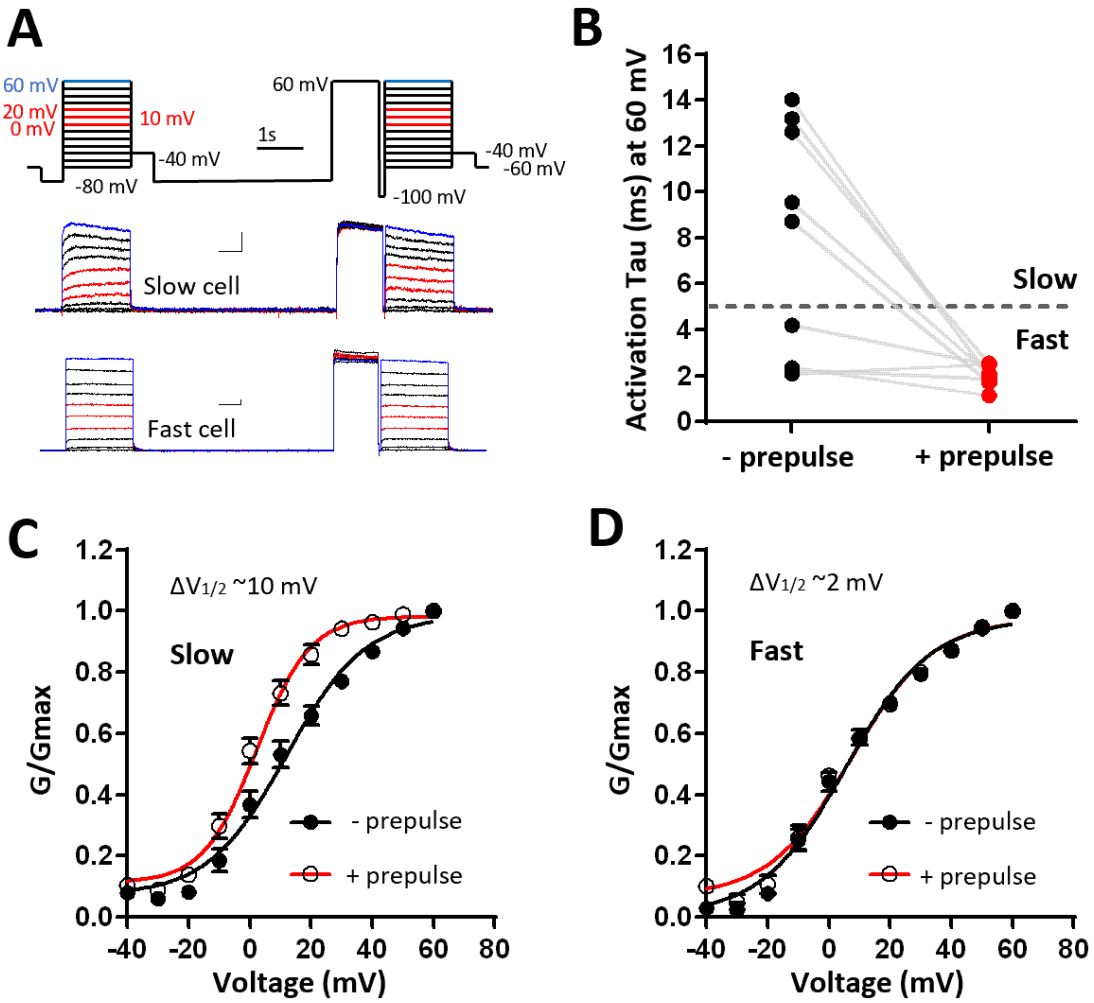

Figure 6: Determination of Kv1.2 activation gating mode. Step protocol for determining Kv1.2 activation gating mode, with representative sample traces for "slow" and "fast" cells (**A**). Activation tau was quantified before and after a 60 mV depolarizing prepulse (**B**). Cells displaying an activation tau > 5 ms were determined to be "slow", and cells displaying an activation tau ≤ 5 ms were determined to be "fast". Slow cells showed a leftward shift in voltage-dependency of activation following the prepulse (**C**). In contrast, and fast cells showed no further potentiation (**D**).

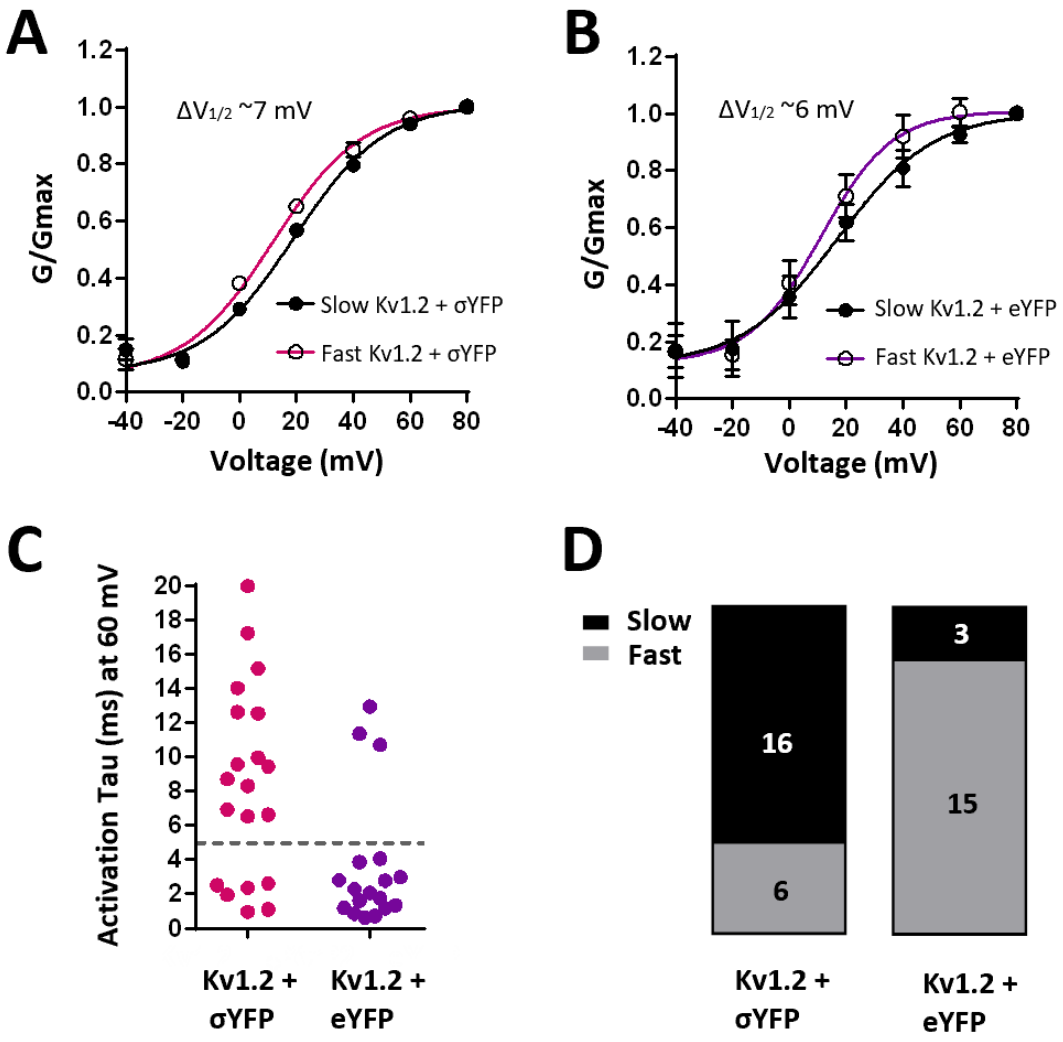

Figure 7: Cells overexpressing Sig-1R are more likely to exhibit "slow" activation gating and cells endogenously expressing Sig-1R are more likely to exhibit "fast" activation gating. Cells expressing Kv1.2 and Sig-1R-YFP (**A**) and Kv1.2 and eYFP (**B**) both displayed "fast' and "slow" cells, with "fast" cells displaying a leftward shift in $V_{1/2}$ of activation. Cells overexpressing Sig-1R showed a higher proportion of cells with an activation tau > 5 ms, and cells endogenously expressing Sig-1R showed a higher proportion of cells with an activation tau ≤ 5 ms (**C**). It was determined that cells overexpressing Sig-1R were more likely to be "slow" and cells endogenously expressing Sig-1R were more likely to be "fast".

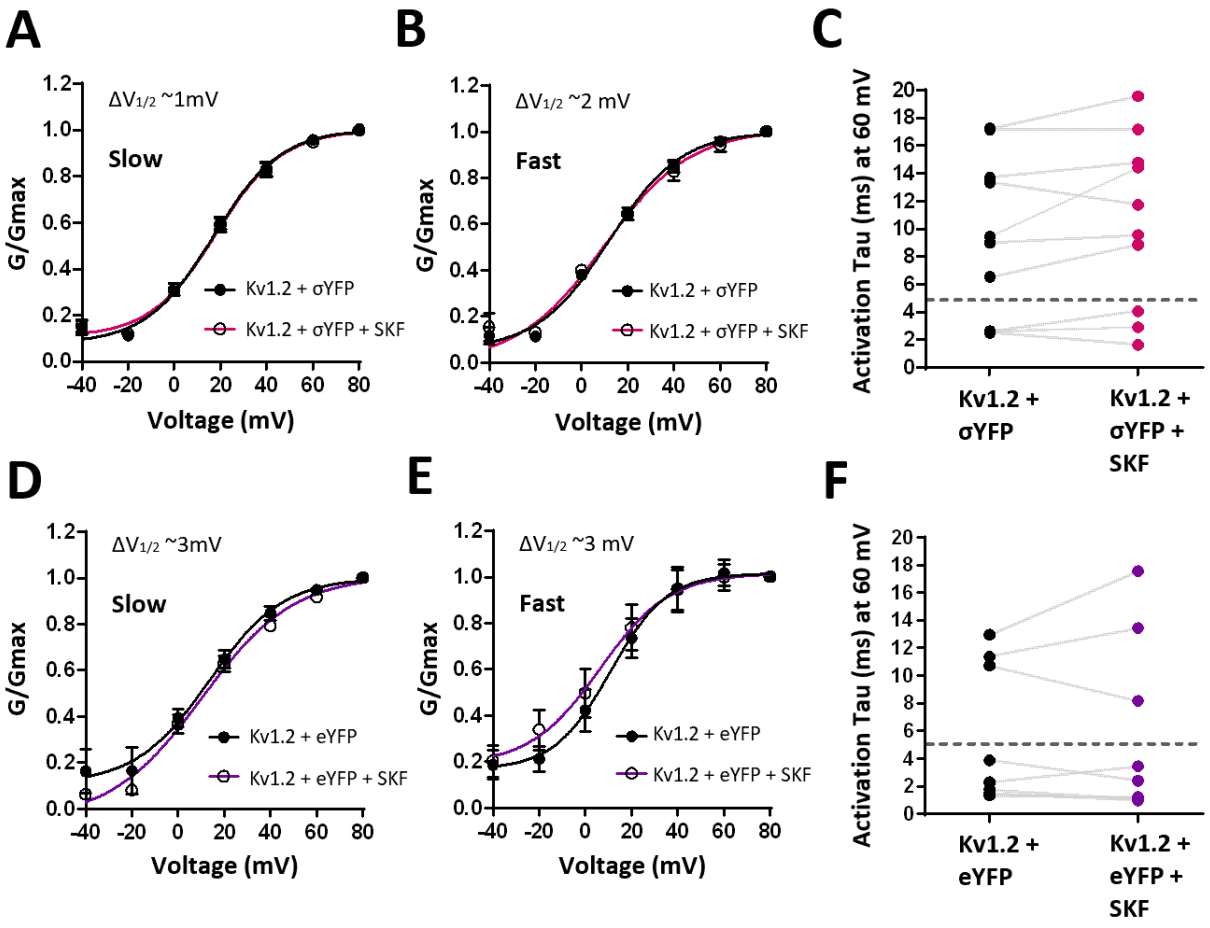

Figure 8: Application of SKF has no effect on Kv1.2 activation gating mode. In cells expressing Kv1.2 and Sig-1R-YFP, application of SKF has no effect on $V_{1/2}$ of activation in "slow" cells (**A**) or "fast" cells (**B**) and has no impact on activation tau (**C**). Similarly, in cells expressing Kv1.2 and eYFP, SKF has no effect on $V_{1/2}$ of activation in "slow" (**D**) or "fast" cells (**E**), or on activation tau (**F**).

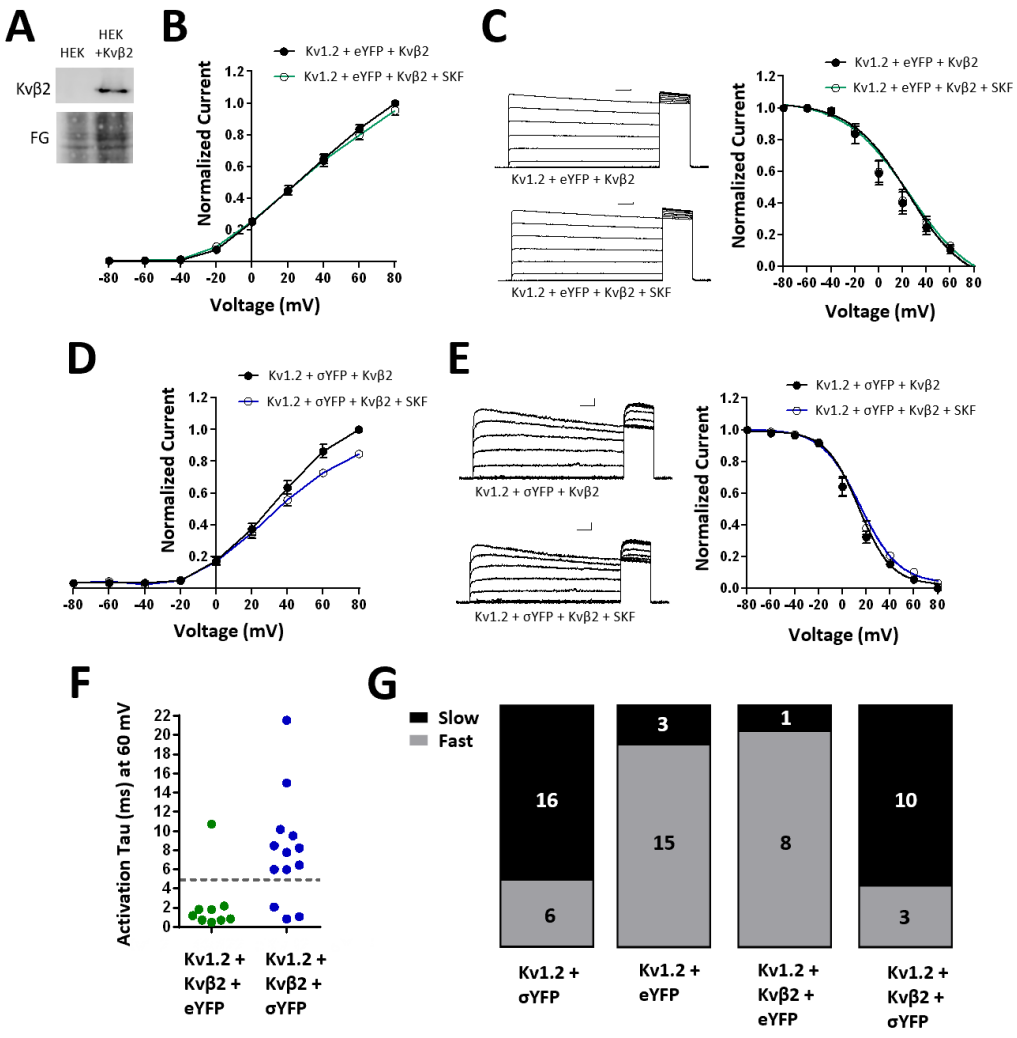

Figure 9: Expression of Kvβ2 blocks the effects of Sig-1R ligand activation on Kv1.2 current amplitude, except when Sig-1R is overexpressed. Western blotting displays expression of Kvβ2 in transiently transfected HEK293 cells (**A**). Voltage-clamp recordings of cells expressing Kv1.2 with Kvβ2 and eYFP displayed no significant decrease in current amplitude upon treatment with SKF (**B**). Voltage dependency of inactivation was calculated from leak subtracted traces, and there was no observed change in $V_{1/2}$ of inactivation (**C**). In contrast, cells expressing Kv1.2 with Kvβ2 and Sig-1R-YFP displayed a significant decrease in current amplitude upon treatment with SKF (**D**). Similarly to all other groups, there was no change in $V_{1/2}$ of inactivation. It was observed that more cells expressing Kv1.2, Kvβ2 and eYFP displayed activation taus ≤ 5 ms at +60 mV, and cells expressing Kv1.2, Kvβ2 and Sig-1R displayed activation taus > 5 ms at +60 mV (**E**). Thus, it was determined that cells endogenously expressing Sig-1R were more likely to be "fast" can cells overexpressing Sig-1R were more likely to be "slow" (**F**). Scalebar in all cases is 500 ms, 300 pA.

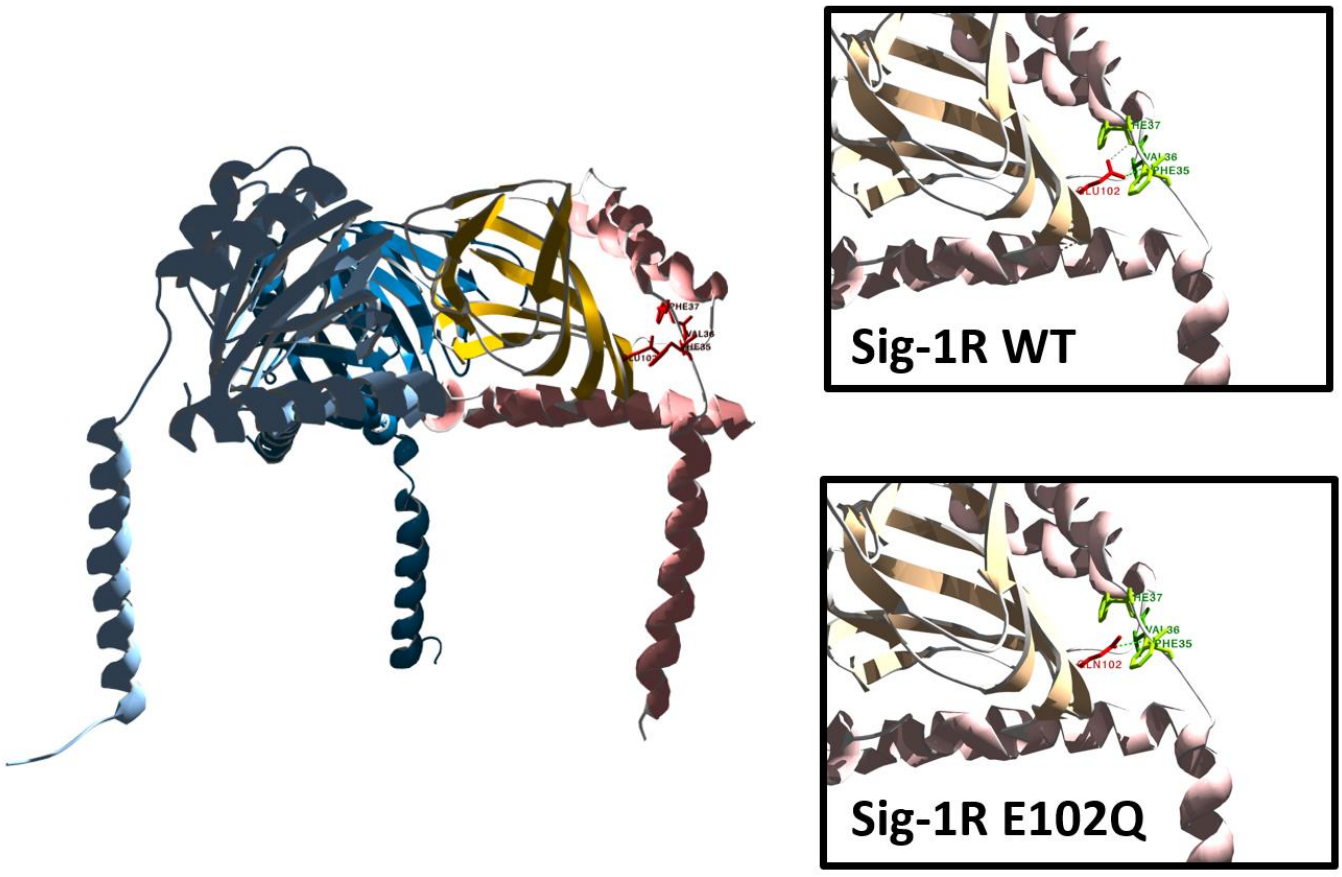

Figure 10: Sig-1R missense mutation results in the loss of a single hydrogen bond. The Sig-1R-E102Q mutation results in the substitution of glutamine for glutamic acid in the linker region between the Sig-1R β2 and β3 regions. *Provided by K. Ferguson, 2016.*

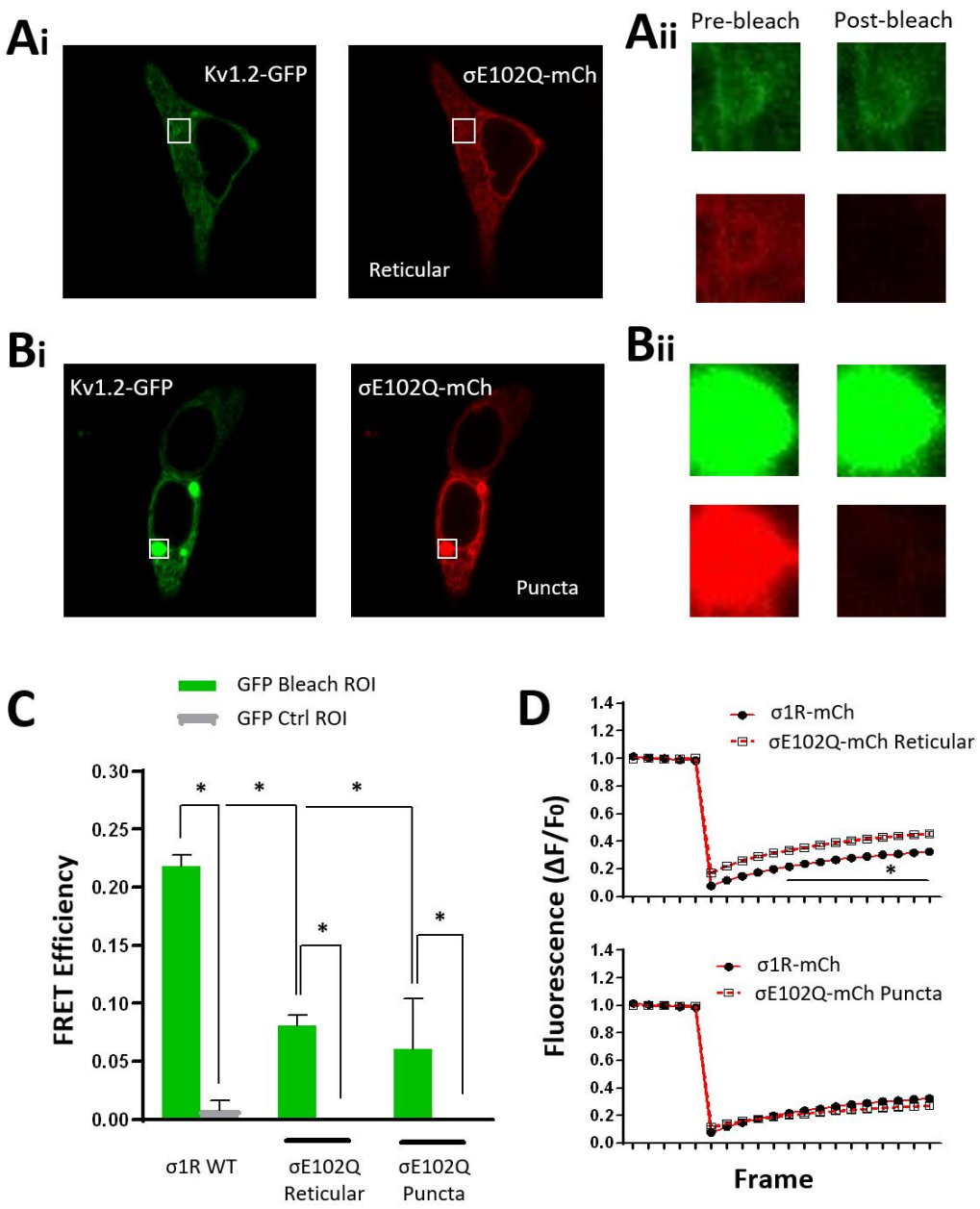

Figure 11: Sig-1R-E102Q shows decreased interaction with Kv1.2 and increased mobility as compared to WT Sig-1R. Representative confocal images of HEK293 cells transiently co-expressing Kv1.2-GFP and Sig-1R-E102Q-mCh, with reticular Sig-1R localization (**A**) and Sig-1R aggregation into puncta (**B**)**,** before and after acceptor photobleaching. Quantification of the images showed a significant decrease of FRET efficiency in both Sig-1R-E102Q groups as compared to WT Sig-1R, and no significant differences between reticular and puncta Sig-1R-E102Q cells (**C**). Reticular Sig-1R-E102Q-mCh displayed increased mobility in FRAP as compared to WT Sig-1R-mCh, but Sig-1R-E102Q-mCh puncta displayed similar mobility to WT Sig-1R-mCh (**D**). Asterisks indicate statistical significance ($p < 0.05$).

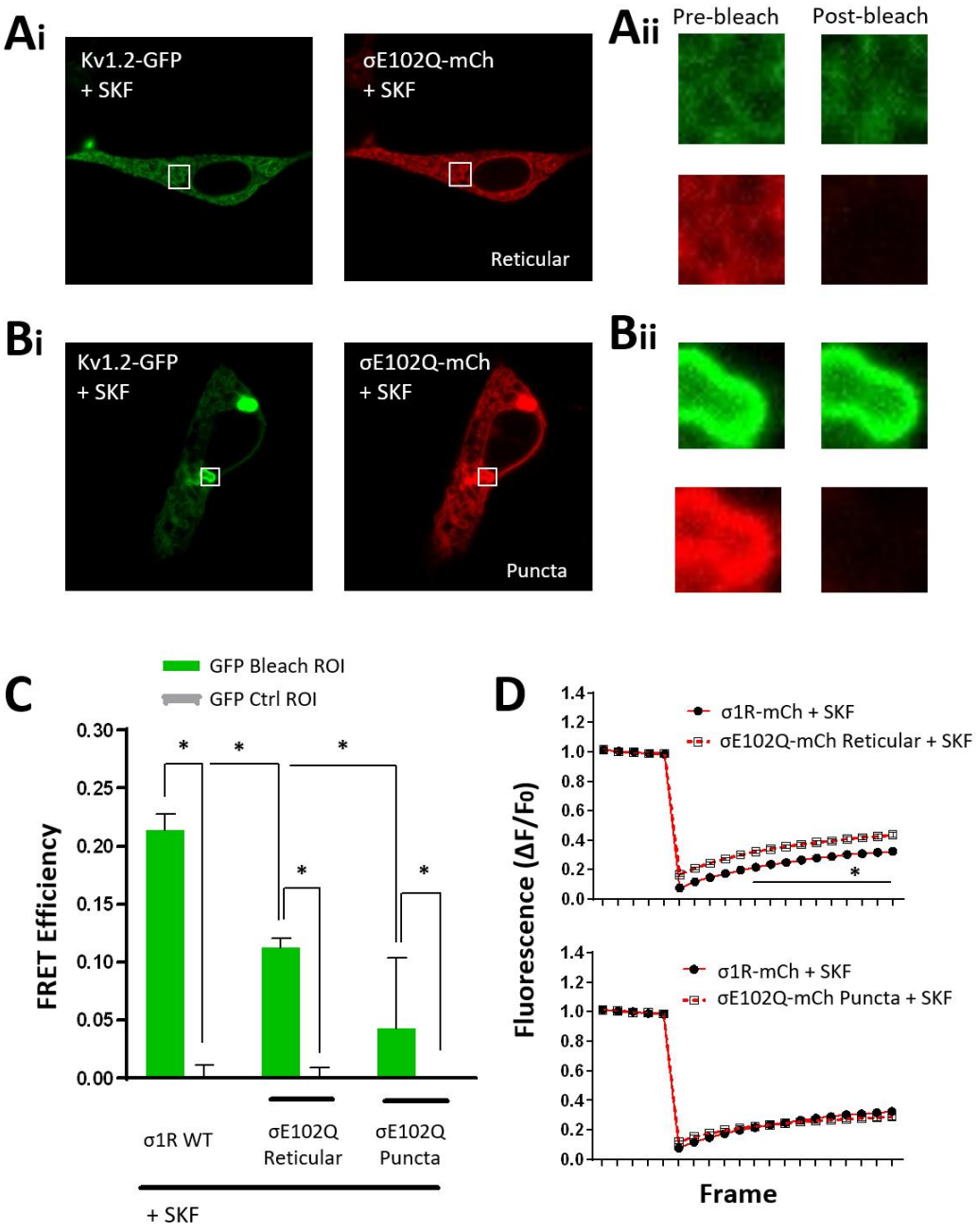

Figure 12: Application of SKF has no effect on Sig-1R-E102Q interaction with Kv1.2 or receptor mobility. Representative confocal images of HEK293 treated with SKF and cells transiently co-expressing Kv1.2-GFP and Sig-1R-E102Q-mCh, with reticular Sig-1R localization (**A**) and Sig-1R aggregation into puncta (**B**)**,** before and after acceptor photobleaching. Quantification of the images showed a significant decrease of FRET efficiency in both Sig-1R-E102Q groups as compared to WT Sig-1R treated with SKF, and no significant differences between reticular and puncta Sig-1R-E102Q cells (**C**). Reticular Sig-1R-E102Q-mCh displayed increased mobility in FRAP as compared to WT Sig-1R-mCh, but Sig-1R-E102Q-mCh puncta displayed similar mobility to WT Sig-1R-mCh (**D**). Asterisks indicate statistical significance ($p < 0.05$).

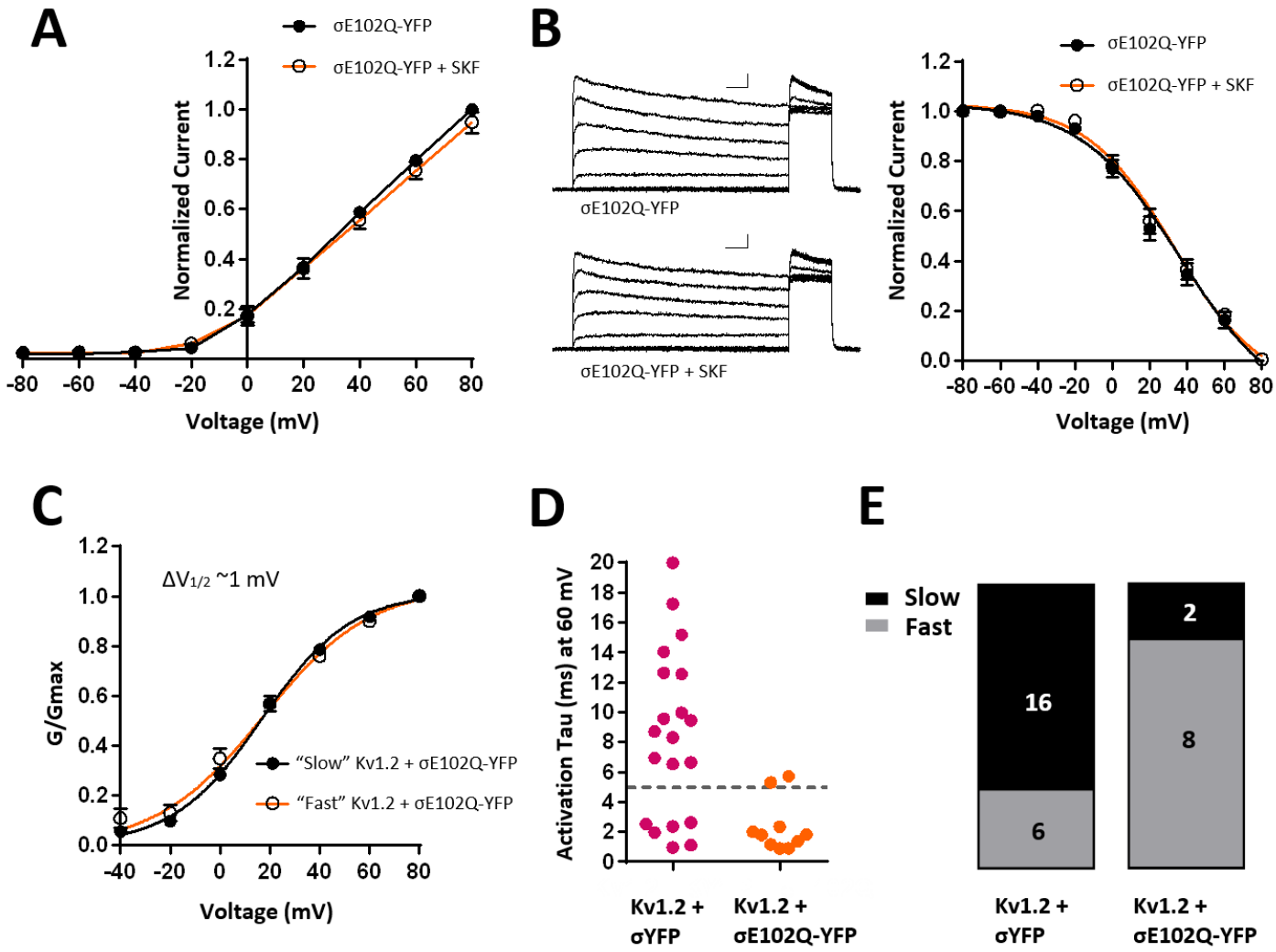

Figure 13: Cells expressing Sig-1R-E102Q show no changes in current amplitude in response to SKF application, and are more likely to exhibit "fast" activation gating. Voltage-clamp recordings of cells expressing Kv1.2 and Sig-1R-E102Q displayed no significant decrease in current amplitude upon treatment with SKF (**A**). Voltage dependency of inactivation was calculated from leak subtracted traces, and there was no observed change in $V_{1/2}$ of inactivation (**B**), as with all other sampled groups. Further, "fast" cells expressing Kv1.2 and Sig-1R-E102Q only exhibited a 1 mV leftward shift in $V_{1/2}$ of activation as compared to "slow" cells (**C**) indicating that the difference between "fast" and "slow" is less pronounced in this group. The majority of Sig-1R-E102Q expressing cells displayed activation taus ≤ 5 ms (**D**) and were more likely to be fast than cells expressing WT Sig-1R-YFP (**E**). Scalebar in all cases is 500 ms, 300 pA.

TABLES

CONSTRCUT NAME	EXPRESSION VECTOR	PLASMID SIZE	SOURCE
Kv1.2	pCMV6	6.4 kB	Origene
Kv1.2-GFP	pLenti-C	8.6 kB	Origene
eYFP	pcDNA3.1/His	4.7 kB	Invitrogen
Sig-1R-YFP	pcDNA3.1/His	5.3 kB	Invitrogen
Sig-1R-mCh	pVLX EF1a	10.1 kB	Addgene
Kvβ2	pCMV6	6.0 kB	Origene
Sig-1R-E102Q-YFP	pcDNA3.1/His	5.3 kB	Invitrogen
Sig-1R-E102Q-mCh	pVLX EF1a	10.1 kB	Addgene

Table 1: List of cDNA constructs used in this study.

Kv1.2 +	Fast Activation Tau			Slow Activation Tau		
	Mean	SEM	n	Mean	SEM	n
Sig-1R-YFP	1.91	0.13	6	13.71	1.99	16
eYFP	2.01	0.28	15	11.68	0.66	3
Kvβ2 + eYFP	1.2	0.22	8	10.7	-	1
Kvβ2 + Sig-1R-YFP	1.31	0.38	3	11.24	1.93	11
Sig-1R-E102Q-YFP	1.53	0.18	8	5.5	-	2

Table 2: Kv1.2 Activation kinetics of all groups at 60mV.